Applicability and long-term safety assessment of geopolymer and cement disposal systems for spent titanate adsorbent from decontamination of wastewater at Fukushima Daiichi Nuclear Power Station

A dissertation submitted in partial fulfillment

of the requirements for the degree of

Doctor of Philosophy in Engineering

by

SOONTHORNWIPHAT Natatsawas

Division of Sustainable Resources Engineering,

Graduation School of Engineering,

Hokkaido University, Japan

2020

Acknowledgement

Foremost, I would like to express my immeasurable appreciation and deepest gratitude to my supervisor, Prof. Tsutomu Sato, who provided me with an excellent opportunity to conduct research at Hokkaido University. His valuable advice, constructive support, and helpful guidance made me complete my research successfully. Moreover, I am always thankful for his patience, kindness, and encouragement throughout my study period. It has been an honor to be his student.

Besides my supervisor, I would like to express my special thanks for acknowledging to Assoc. Prof. Tsubasa Otake and Asst. Prof. Ryosuke Kikuchi, for the recommendations, academic assistance, and moral support for this study. My sincere thanks are also extended to Prof. Naoki Hiroyoshi and Assoc. Prof. Yogarajah Elakneswaran, served as committee members of my annual thesis evaluation and thesis defense, for their valuable advice and insightful comments that considerably improve my works.

I thank my fellow labmates and technicians in the Laboratory of Environmental Geology, Graduate School of Engineering, Hokkaido University, for the stimulating discussion and teaching me to use the instruments. I also give thanks to our laboratory's secretary, especially Yoshie Hoshi, to help me organize all issues during the study life. Friendship and good collaboration happen here, and it was a great time with all of you during my three-year life in Japan.

A debt of gratitude is also owed to Asst. Prof. Naoya Sakamoto, Creative Research Institution, Research Department, Hokkaido University, for help with using isotope microscope. Also, the author is appreciative to the persons who relate to aid for pointing, helping, and providing guides to obtain the results toward completing this study.

I am deeply grateful to JICA Innovative Asia Scholarship for the precious financial support to study here. Besides, thanks to Fortum Power and Heat Oy company to provide the SrTreat® for using in the experiments.

Last but not least, I am forever express my profound thankfulness to my parents and my family, who instilled in me the virtues of commitment. Without you, none of this would indeed be possible.

Abstract

Since the accident at Fukushima Daiichi Nuclear Power Station (FDNPS) in March 2011, the contaminated water with radionuclides has been continuously produced by the cooling process of damaged nuclear fuel. Among various radionuclides present in the wastewater, ^{90}Sr and $^{137,134}Cs$ are the important contaminants that have to decontaminate due to their long half-life and effect on human bodies. Therefore, ion-exchange methods for decontamination and reduction of these radionuclides of wastewater have been carried out using absorbents. For instance, Simplified Active Water Retrieve and Recovery System (SARRY) and Advanced Liquid Processing System (ALPS) in FDNPS uses engineered zeolites and commercial hydrous sodium titanate as an ion exchanger for reduction of radioactive Cs and Sr concentration, respectively. Concentrate on titanate adsorbent, which has been used for Sr removal, significant quantities of these spent adsorbents have been repeatedly accumulated. They have been contemplated the way for safe storage and disposal of titanate adsorbent, and these come to be an urgent issue in FDNPS. Therefore, there is a critical challenge to find out a material for stabilizing those adsorbents to ensure long term safety and disposal. Alkali-activated materials (geopolymers) are hypothesized as a candidate for forming waste form to carry out this consolidation. The stabilization and potential for radionuclide immobilization of K-based geopolymer embedded titanate adsorbent were investigated in this study.

Chapter 1 refers to the background, objectives of this study. The stories that happen after the accident were narrated. This chapter also describes the advantages and drawbacks of each kind of waste form and clarifies the reason for giving precedence to alkali-activated materials (geopolymer) in this study. Furthermore, the objectives and outline of the dissertation are detailed.

Chapter 2 presents the literature reviews on geopolymer waste and the absorption of Sr and Cs by titanate. To catch up on the knowledge of fundamental mechanisms on geopolymerization, express the utility of geopolymer, and comprehend Sr and Cs' sorption mechanisms on titanate adsorbent.

In Chapter 3, leaching experiments and observations of Sr distribution of spent titanate adsorbent embedded in geopolymers, loaded with Sr at realistic concentrations, were conducted. The experimental results illustrate that only 0.75 % of the Sr was leached from a K-geopolymer loaded with 30 % (by solid weight) of spent adsorbent after 360 days of immersion in deionized water.

Most of Sr remained in the geopolymer even after 360 days. From the observations of Sr distributions by electron and isotope microscopy, Sr remained in the titanate adsorbent and did not diffuse into the geopolymer matrix. Leaching of Sr (loaded at a similar concentration) from the K-geopolymer without the adsorbent was also limited, only 0.05 % after 360 days of leaching. Both titanate adsorbent in K-geopolymer matrix, and the K-geopolymer itself, offer attractive potential for Sr immobilization.

Chapter 4 investigates the adsorption behavior of Cs with titanate adsorbent as an optional method for removing Cs in contaminated water. Leaching experiments and observations of the Cs, the distribution of spent titanate adsorbent embedded in geopolymers were also conducted. 6.92% of Cs leached from a K-geopolymer loaded with spent adsorbent after 360 days of leaching. Ascribed to the prominent content of K inside, the system can potentially influence and exchange with Cs on both titanate adsorbent and possibly on geopolymer binder. Moreover, the leaching experiments revealed high leachability of Cs from the matrix binder, while adsorbed Cs on titanate adsorbent prior insert into the matrix could suppress Cs leachability. In order to further develop and apply for the real situation, using titanate adsorbent becomes the other method for immobilization Cs in the geopolymer matrix.

Chapter 5 estimates the safety assessment of geopolymer waste with titanate adsorbent loaded Sr and Cs. The safety assessment system is used for evaluating the suitability of waste form for long-term storage and disposal in the different disposal types simulated form GoldSim software by using the actual numerical value from a real situation and leaching rate (90 days leaching). The safety evaluation conducted here reveals that it is practical to utilize pit type disposal system for the solidified geopolymer with titanate adsorbent generated in the treatment of contaminated water processes. With the target radionuclides (Sr-90), it was confirmed that the maximum annual exposure dose was below the limit of standard-dose in both examined cases as groundwater transfer scenario and land-use scenario. On the contrary, a disposal system for the solidified geopolymer with titanate adsorbent is not suitable to adopt the trench type.

Chapter 6 provides general conclusions and recommendations for future necessities and suggestions for research. In short, this study examines the encapsulation mechanisms of the low concentration Sr and Cs in the titanate adsorbent within metakaolin based geopolymer. Titanate adsorbent adsorbed Sr and Cs are simulate the actual situation from the reprocessing of

contaminated water in FDNPS. This study also brought the leaching rates and the distribution of Sr and Cs on the matrix and suggested that K-geopolymers are excellent candidates as a waste matrix destined for long term storage and disposal of spent titanate adsorbent. This study also provided the possible way to safe storage and disposal and admitted that the geopolymer matrix embedded the spent titanate adsorbents adsorbed strontium is suitable and safe in the shallow underground pit disposal system. Lastly, with the aim of further develop and apply these titanate adsorbents with K-based geopolymer binder. The aspects that need to be considered are the in-depth details of adsorption mechanisms and the structure of solidified specimens, also, examine the leaching rates from different types of leachant.

Table of Contents

List of Tables

List of Figures

Chapter 1: General introduction

1.1 Background

The 9.1 magnitude earthquake accident occurred near the northeast coast of the Tohoku region in Japan at a depth of 15.2 miles on March 11, 2011, resulting in the followed shortly after a 30-foot wave tsunami, which has tremendous damage to human life and properties. Owing to that catastrophe, the Fukushima Daiichi Nuclear Power Station (FDNPS), located in Okuma city, Fukushima prefecture, which is owned and operated by Tokyo Electric Power Company (TEPCO), disabled all-electric power which is destroyed the generators and system in the plants. The nuclear reactors automatically shut down, while the nuclear fuel requires continued cooling because residue fission products continue to decay and produce a large amount of heat, thus, cooling down the nuclear reactors by water injections was ongoing (Shibata et al., 2012). The massive amount of contaminated water with significant radioactive elements such as cesium-137/134 and strontium-90 was inevitably produced and necessary to decontaminate the water to enable repeated use due to the limited storage capacity.

Cesium-137/134 is the dominant radionuclide contained in the contaminated water. The treatment system for the contaminated water had specific requirements to achieve high decontamination factors. At FDNPS, the treatment system to reduce the amount of cesium/strontium radioactivity is the Circulating Water Cooling System and Simplified Active Water Retrieve and Recovery System (SARRY), which used of engineered zeolites for Cs and silicotitanate for Sr. Following these systems, the radioactive elements still remains in the reactor, the other treatment facilities such as Advanced Liquid Processing System (ALPS) was installed to reduce 62 radionuclides including strontium-90 to the non-detectable level (Kirishima et al., 2015). Strontium-90 was diminished by using the highly selective material (SrTreat) as an adsorbent, which results in the high efficiency and high decontamination factor of radioactive strontium removal (Tusa, 2014).

SrTreat is an inorganic ion exchanger which structure is based on sodium titanate, consisting of layered edge-sharing TiO_6 octahedral chains linked with exchangeable interlayer sodium cations. After reacting with strontium, large volumes of the spent adsorbent loaded with strontium have been stored in a temporary radioactive waste storage site awaiting conditioning for solidification prior to the disposal. The solidification purposes for the efficient encapsulation and economical long-term safe storage of strontium to not leach out to affect the environment.

Secondary nuclear wastes for stabilizing and disposing of spent adsorbents have been investigated, the currently available options such as vitrification, solidification with cementitious materials, and solidification with alkaline activated materials, are being considered. The vitrification requires the destruction of the adsorbent granules, involves the thermal treatment, and yields a waste form that can perform well in high radioactivity situations with stable chemical conditions for the waste disposal and management. However, the required deep geological disposal, detrimental characteristics of incineration processes, and unavoidable generation of gases present drawbacks for this process (International Atomic Energy Agency, 2002). Conventional cementitious materials, which are simple to produce and apply, cause minimal secondary waste generation, and become an attractive option in such situations. At the same time, the generation of greenhouse gases in cement manufacture, and the high free water content which may induce problematic hydrogen generation, low resistance to acid and fire conditions, and incompatibility with several types of waste have been noted as disadvantages of conventional cementitious materials (Atkins and Glasser, 1992), (Mehta and Monteiro, 2014).

A further treatment option is offered by alkaline activated cementitious materials, which are a type of innovative materials also known as “geopolymers”, which can be designed to include desirable properties such as excellent thermal resistance, high and durable performance characteristics, and stability against chemical attack, as well as low content of free water, and reduced greenhouse emissions in the manufacture (Khalil and Merz, 1994). However, the somewhat complex manufacturing procedures and the geopolymerization process’s sensitivity to parameters such as water content remain issues of concern in practical application to nuclear industry problems (Jang et al., 2017). The acceptance criteria used for considering the selection of a solidified form of waste include adequate chemical and physical stability for storage and disposal that it is possible to produce the material economically, and that secondary waste generation during the production processes is minimal (International Atomic Energy Agency, 2002). Considering all the above, an alkaline activated material was investigated in this study as a potential class of cementitious materials used in conditioning and solidifying spent titanate adsorbents.

1.2 Objectives

This study focused on investigating the leaching behavior and encapsulation mechanisms of strontium and cesium in titanate adsorbent embedded in a K-based geopolymer waste form. Considering a trace concentration of non-radioactive strontium and cesium loaded in the SrTreat replicating the actual conditions and applying alkali-activated metakaolin with potassium silicate activator as the waste matrix for encapsulation of the adsorbent. Furthermore, the comparison of leaching rate and mechanisms of strontium and cesium from geopolymer waste form and cementitious material with/without adsorbent were elucidated by conducting leaching experiments in deionized water, and microanalysis of the specimens after different leaching periods. Finally, the applicable and suitable disposal type for long-term safe storage of the solidified waste form simulated by GOLDSIM software was proposed.

1.3 Outline of the dissertation

This dissertation is composed of six chapters. First, the background, research objectives of this study, an outline of the dissertation are described in chapter 1. Following this, the related literature review on geopolymer waste and adsorption of strontium and cesium by titanate supporting and explaining the basis of the experiments are discussed in chapter 2. Then, two topics are considered in this dissertation. To begin with, “Encapsulation of Sr-loaded titanate spent adsorbent in Potassium Aluminosilicate geopolymer” (Chapter 3), investigates the leaching behavior of strontium in titanate adsorbent embedded in geopolymer waste form and suggests the encapsulation mechanisms of strontium. Subsequently, the leaching behavior of cesium also examines in chapter 4, “Encapsulation of Cs-loaded titanate spent adsorbent in Potassium Aluminosilicate geopolymer” for cesium mechanisms which happened inside the waste form. Both chapters also compared the behavior of each radionuclide when it is embedded in different kinds of waste, such as geopolymer waste form without titanate adsorbent, Ordinary Portland cement with titanate adsorbent, and Ordinary Portland cement without titanate adsorbent. In chapter 5, the safety assessment of geopolymer waste with titanate adsorbent was proposed. Finally, chapter 6 gives a summary and general conclusion of all results as well as a viewpoint for future works and recommendations.

Chapter 2: Literature review on geopolymer waste and adsorption of Sr and Cs by titanate

2.1 Geopolymer waste

Davidovits introduced a geopolymer in the 1970s, which has source materials that provide silicon (Si) and aluminum (Al) for reaction by an alkaline activator solution. Followed by curing at an ambient or slightly higher temperature, to formation the process in terms of geopolymerization reaction. The empirical formula of geopolymer as expressed in the formula of:

$$M_n\{-SiO_2)_z - AlO_2\} \cdot wH_2O$$

M is a cation such as K^+, Na^+; n is the degree of polycondensation; z is the Si/Al molar ratio, and w is the amount of binding water.

The main precursors as the aluminosilicate sources used to produce alkali-activated materials are fly ash, blast furnace slag (BFS), and metakaolin, which provide Si^{4+} and Al^{3+} ions in the geopolymer binding system. Tetrahedral SiO_4 and AlO_4 are linked by sharing oxygen atoms under the term poly(sialate), where sialate is an abbreviation of silico-oxo-aluminate (Figure 2-1). Then, a negative charge leaves in the IV-fold coordinated Al that is charge-balanced by cations. An alkaline silicate solution usually gives the cation, a mixture of alkali hydroxides (NaOH or/and KOH) and alkali silicate solution, known as a water glass (Na_2SiO_3 or/and K_2SiO_3). The alkali hydroxide is required for the dissolution of aluminosilicates to form solid binder product while alkali silicate solution acts as binder and activator to accelerate the reaction (Abdullah et al., 2018), (Provis and Bernal, 2014), leading to a final structure represented in Figure 2-2. The initial setting takes a few hours and a relatively stable microstructure depending on the precursor characteristics and curing temperature.

The mechanisms of geopolymerization purposed by Duxson et al. (2007), shown in Figure 2-3, outlines the fundamental processes occurring in the transformation of a solid aluminosilicate source into an alkali aluminosilicate. Also, the chemistry of alkali-activated binders is crucial to classify according to the primary type of gel that governs the structure mainly on the basis of calcium content in the system, the process, and reaction products of a solid aluminosilicate precursor as shown in Figure 2-4. Deficient calcium is often presented as N,K-A-S-(H), the H is shown in parentheses to indicate that water is not a major structural component of this gel. While

the C-A-S-H types gels, which are domains calcium content, always coexist with secondary products of the layered double-hydroxide group (Provis and Bernal, 2014).

Any source of silica and alumina that can be dissolved in an alkaline solution can act as a geopolymer precursor. The different SiO_2, Al_2O_3, and CaO mass contents are shown in Figure 2-5. Metakaolin is considered as a raw material for making geopolymer in this study.

The silica, aluminum, alkali, and water were brought to the mixture by the raw materials, allowing the total formulation of a geopolymer. Figure 2-6 presents the filled contour plot made by Kamalloo et al. (2010), which indicates the effect of R_2O/Al_2O_3 (where R=Na or K), SiO_2/Al_2O_3, and H_2O/R_2O molar ratios on the compressive strength of metakaolin-based geopolymers. The results show that the optimized SiO_2/Al_2O_3, R_2O/Al_2O, and H_2O/R_2O ratios to achieve high compressive strength (up to 80 MPa) should be 3.6-3.8, 1.0-1.2, and 10-11, respectively. It reveals that increasing the H_2O/R_2O ratios, which corresponds to increasing the amount of water, drastically lowers mechanical performance.

The formulation parameter affects the mechanical performance of a geopolymer and also other properties. Duxson et al. (2005) have published SEM micrographs of geopolymers exhibiting significant changes in their microstructure with variations of the Si/Al ratio. A Si/Al molar ratio of 1.4, some unreacted solid aluminosilicate remains, and the more the molar ratio increases, the more homogeneous the structure becomes, with a significant change between 1.45 and 1.60, as can be seen on Figure 2-7.

Geopolymers express excellent mechanical and physical properties, such as harden rapidly, low density, good chemical, thermal stability with low shrinkage, high mechanical strength, high perseverance in acidic and alkaline media, low CO_2 construction materials (Bernal and Provis, 2014), therefore, they are widely applied in various fields as new materials with high tech application. Geopolymer has been used in several fields such as molding, tooling, building thermal insulation, and furnace insulation. Besides, geopolymers have been used to produce high-quality brick and tiles, aircraft composites, cabin interiors, lightweight materials, sound insulating materials. Especially, geopolymers have molecular structures that resemble zeolitic materials, which can immobilize, incorporate, and retain toxic waste or heavy metals as they can adsorb and solidify toxic chemical waste (Abdullah et al., 2018).

2.2 Adsorption of Sr and Cs by titanate

The SrTreat® used in the experiments is a highly selective inorganic ion exchanger for strontium whose structure is based on a sodium titanate. Conceptually, it is composed of a layer structure of a titanium-oxygen octahedral sheet with exchangeable sodium cations located in the interlayer (Lehto et al., 1999). These sodium ions are readily exchangeable, and the layered structure gives a large surface area with a high amount of interlayer water and a relatively open layered structure. These characteristics support the efficiency of the ion exchange reaction between Na^+ and other more-preferred cations (Lehto and Clearfield, 1988), (Tusa et al., 2014), (Ide et al., 2014). Valence, hardness, and radius of cations are the main factors to determine the selectivity. Sr^{2+} has a higher valence than that of Na^+, and the substitution of multivalent for monovalent cations will decrease the number of ions between the interlayer of the titanate sheets and will lead to a shrinking of the layer spacing making the layered structure more stable (Ali, 2004), (Villard et al., 2015), (Wen et al., 2016). In the case of Cs^+, the replacement of monovalent Na^+ by other monovalent could be discussed according to Pearson's Hard-Soft-Acid-Base (HSAB) theory, which hard acids react strongly to hard bases, and soft acids react strongly to soft bases. As H_2O in the interlayer of titanates are a hard base and bind tightly to Na^+, the exchange of Na^+ by a lower hardness value (e.g., Cs^+) is always followed by dehydration which also leads to the collapse of the layered structure. The collapse of the layered structural results the immobilization of cations inside the interlayer, and cause the irreversible ion exchange (Li et al., 2012). These characteristics make the adsorption of Sr^{2+} and Cs^+ on titanate adsorbents highly selective when compared to Na^+, almost all of the Sr^{2+} and Cs^+ exchangeable with Na^+ in the sorbent with remaining Na^+ mainly left on the titanate adsorbent as expressed in equation 2-1 and 2-2, respectively.

$$Na_aTi_bO_c + n\ Sr^{2+} \rightleftharpoons Na_{a-2n}Sr_nTi_bO_c + 2n\ Na^+ \quad (2\text{-}1)$$

$$Na_aTi_bO_c + n\ Cs^+ \rightleftharpoons Na_{a-n}Cs_nTi_bO_c + n\ Na^+ \quad (2\text{-}2)$$

Protons released through water self-ionization can also participate in ion exchanges, resulting in a protonated or hydrated product of titanate adsorbent as expressed in equation 2-3. Here the H^+ is a small cation that is strongly adsorbed since it can move close to the active site of the adsorbent and obstruct the ion exchange with Sr^{2+} and Cs^+. Therefore, low pH systems are not suitable for this adsorbent. This is the reason high pH systems such as geopolymers and cementitious matrices

are proposed to hold the Sr ions in the interlayer structure of the titanate (Lehto and Clearfield, 1987), (Lehto et al., 1999).

$$Na_aTi_bO_c + x\ H_2O \rightleftharpoons Na_{a-x}\ H_xTi_bO_c + x\ Na^+ + x\ OH^- \qquad (2\text{-}3)$$

Three factors are affecting the ion exchange for predicting the selectivity of competing cations on titanate adsorbent. The cations with higher valence, lower hardness, and smaller radius will be more preferred. The hardness and radius values of some related cations tabulate in Table 2-1 for comparing these values of two competing cations.

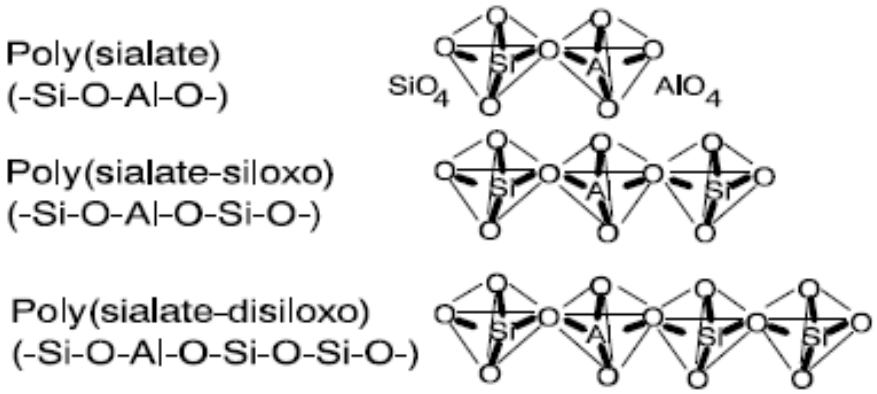

Figure 2-1 Geopolymer terminology (Davidovits, 1994)

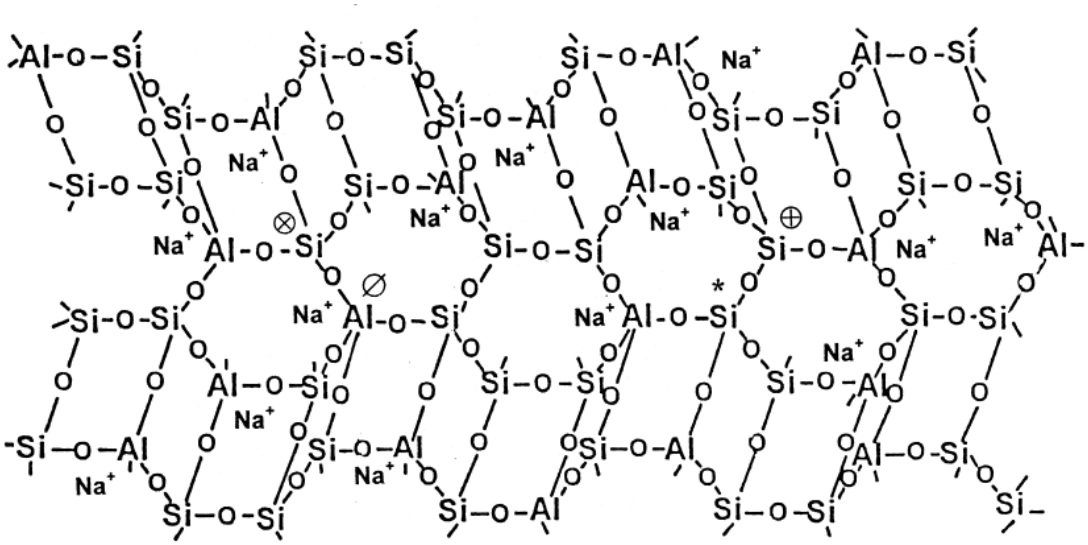

Figure 2-2 Three-dimensional framework structure for Na-polysialate polymer (Barbosa et al., 2000)

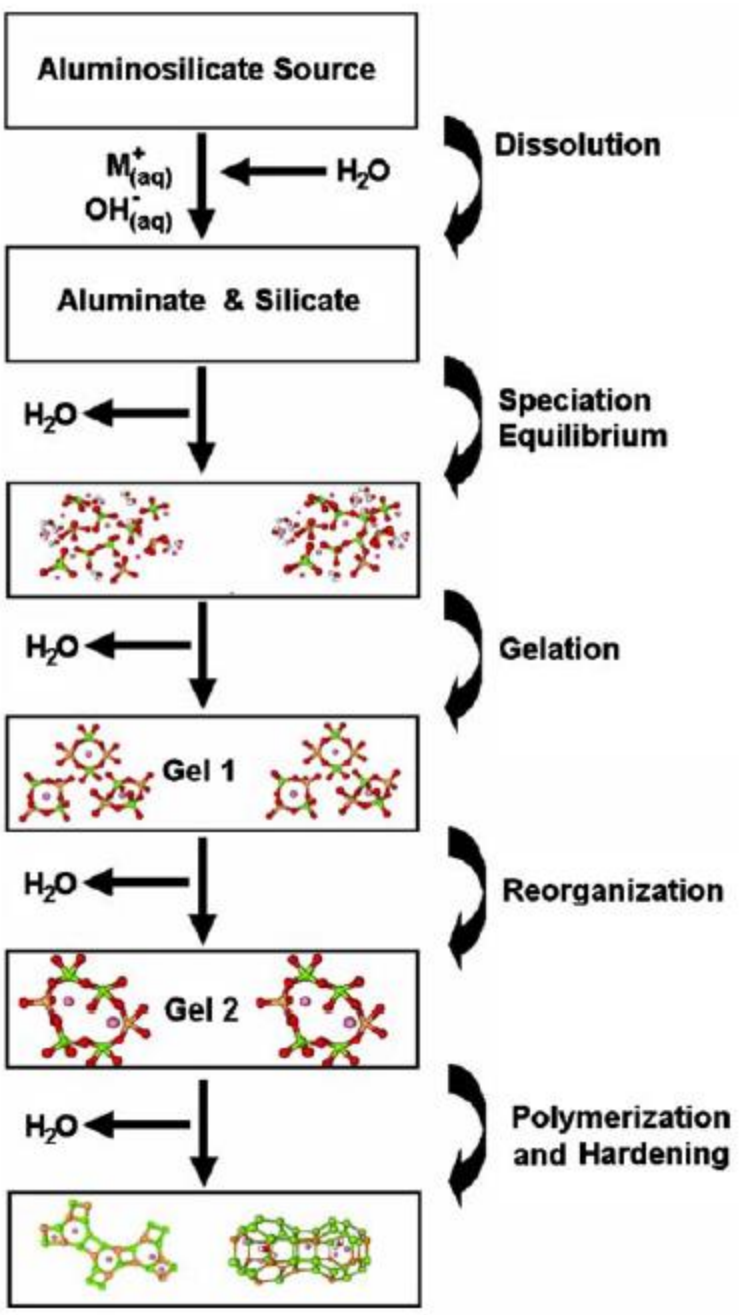

Figure 2-3 Reaction mechanisms for geopolymerization (Duxson et al., 2007)

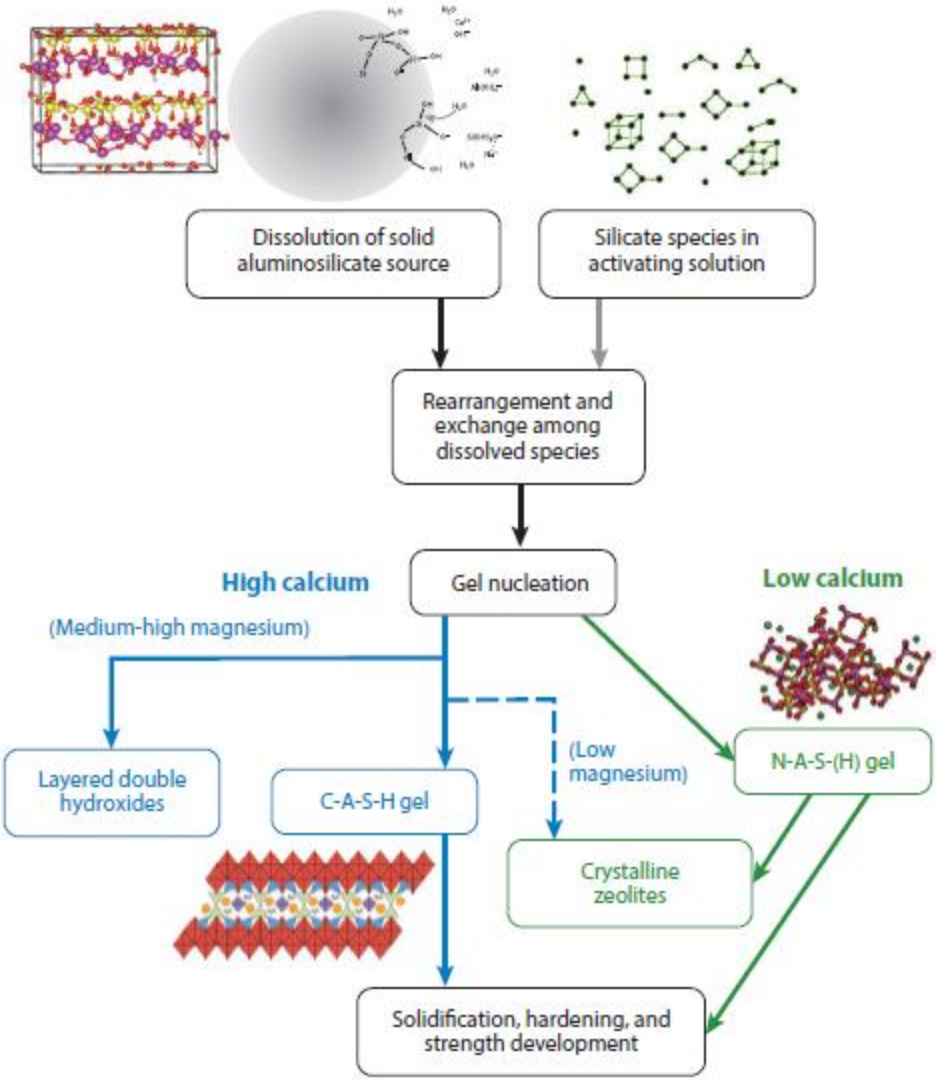

Figure 2-4 Process and reaction products of alkaline activation of a solid aluminosilicate precursor (Provis and Bernal, 2014)

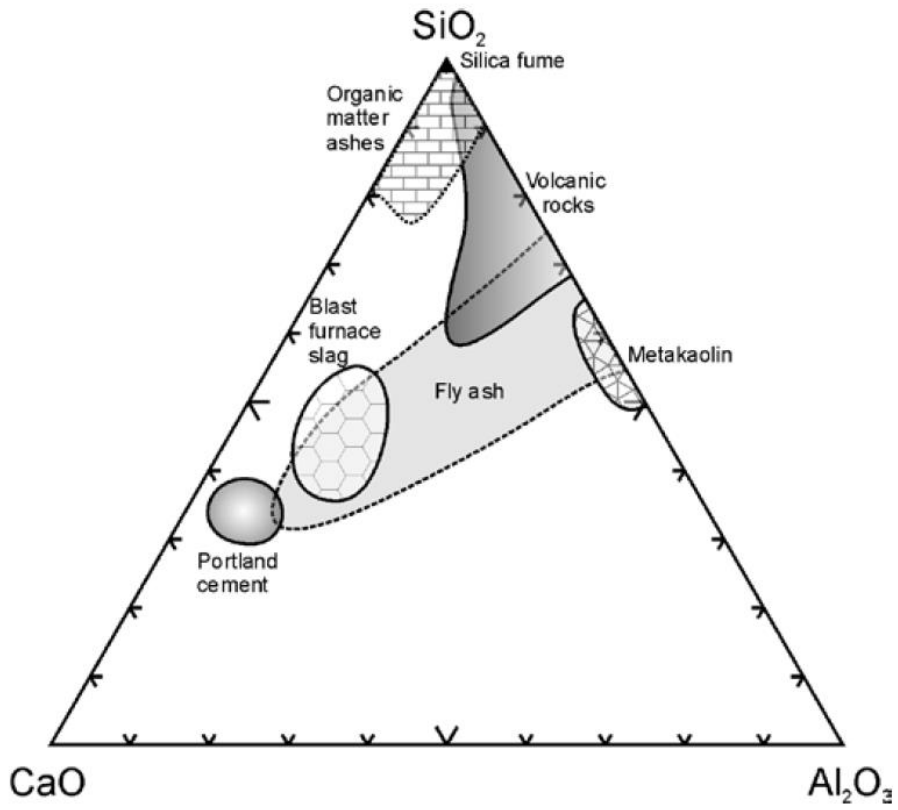

Figure 2-5 Ternary CaO-SiO_2-Al_2O_3 diagram (wt%) of the major cementitious materials (Snellings et al., 2012)

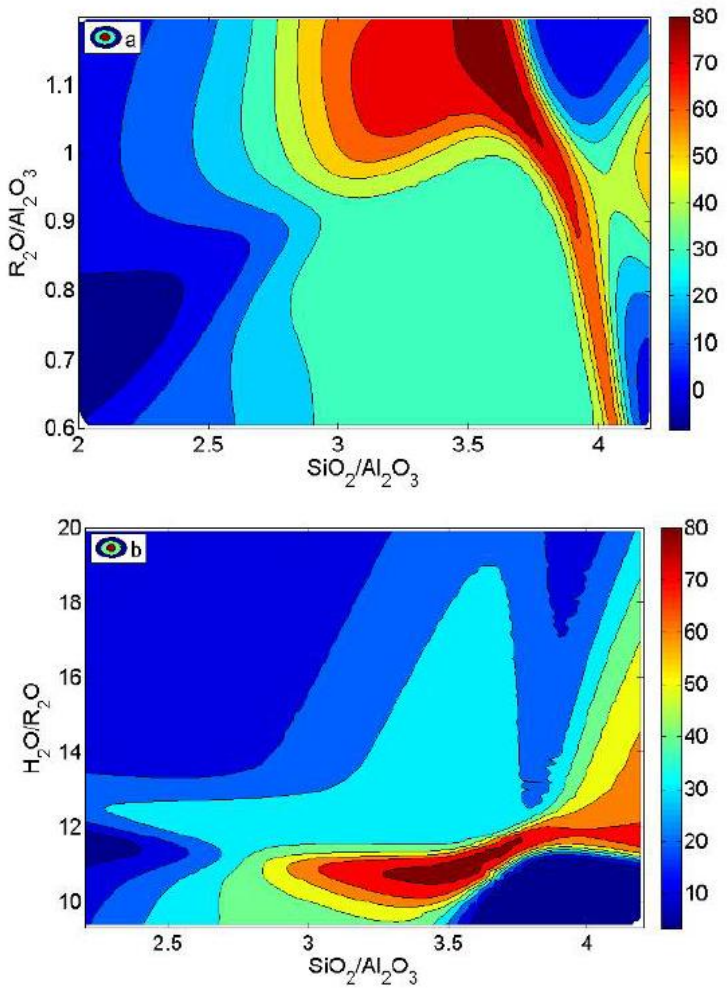

Figure 2-6 Filled contours plot of compressive strength (MPa) showing the effect of R_2O/Al_2O (where R=Na or K), SiO_2/Al_2O_3, and H_2O/R_2O molar ratios (Kamalloo et al., 2010)

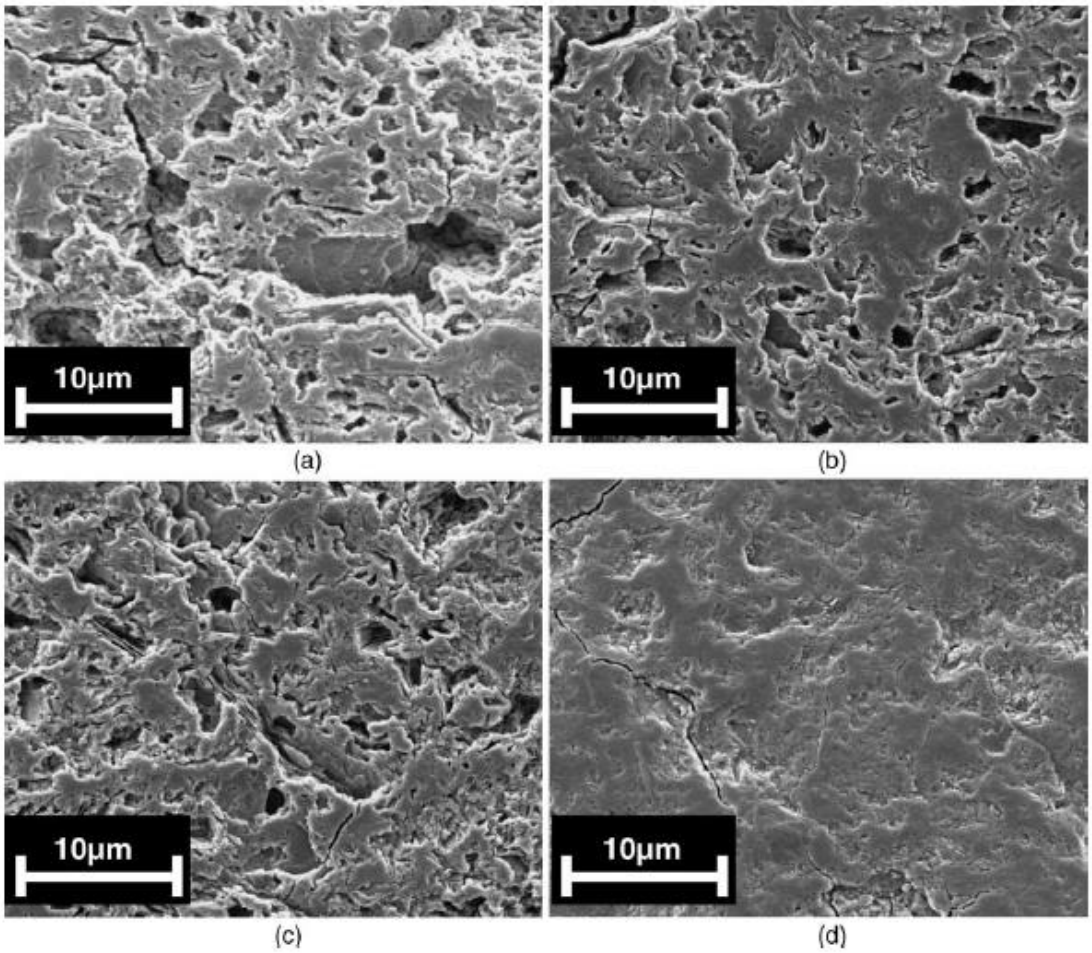

Figure 2-7 SEM micrographs of geopolymers with Si/Al = (a) 1.45, (b) 1.50, (c) 1.55 and (d) 1.60 (Duxson et al., 2005)

Table 2-1 The value of absolute hardness and radius of some related cations

Cations	Absolute hardness (Pearson, 1988)	Radius (Å) (Shannon, 1976)
H^+	∞	0.18
Na^+	21.1	1.02
K^+	13.6	1.38
Cs^+	10.6	1.67
Ca^{2+}	19.5	1.00
Sr^{2+}	16.3	1.18

Chapter 3: Encapsulation of Sr-loaded titanate spent adsorbent in Potassium Aluminosilicate geopolymer

3.1 Introduction

Since the Fukushima Daiichi Nuclear Power Station (FDNPS) was significantly damaged the 2011 high magnitude earthquake and consequent tsunami, a huge amount of water has been injected to cool the resulting fuel debris. This coolant water is contaminated with radionuclides from inside the nuclear reactor, and it has therefore been necessary to decontaminate the water to enable repeated use of the water in the circulating water-cooling system that was established. In the decontaminating/circulating system, sodium titanate as an inorganic ion exchanger has been used to absorb and remove radionuclides, especially ^{90}Sr, from contaminated water with a high decontamination factor in the recirculating system. High removal efficiency has been demonstrated for Sr by sodium titanate compounds (Izawa et al., 1982), (Tusa, 2014), (Tusa et al., 2014), (Villard et al., 2015), (Kirishima et al., 2015). However, large volumes of the spent adsorbent loaded with Sr have been stored in a temporary radioactive waste storage site at the FDNPS, awaiting conditioning for solidification prior to the disposal.

Suitable methods for encapsulation and long-term safe storage of these spent ion exchanger adsorbents have been investigated to determine the formation of monolithic solidified waste forms, as a key requirement for any conditioning process. Geopolymers, a type of alkaline activated material, is a prominent option material which is synthesized by the reaction between an aluminosilicate precursor and an alkaline activator through a process involving dissolution, polycondensation, and hardening (Škvára et al., 2006), (Provis, 2014). The resulting AlO_4-SiO_4 structure of the geopolymer that forms during the rearrangement process results in a net negatively charged framework (as in other aluminosilicate frameworks, zeolites), where cations needed to balance the charge, and the structural similarity of geopolymers to zeolites makes them candidates to participate in ion exchange with charge balancing cations (O'Connor et al., 2010), (Gasca-Tirado et al., 2018). This differs from the behavior of conventional cement systems, where the hydraulic binder is dominated by calcium silicate hydrate (C-S-H). The microporous structure and highly alkaline pore solution in hardened cement systems (conventional and geopolymer) are effective in the immobilization of radionuclides (Atkins and Glasser, 1992), (Shi and Spence, 2004), (Bart et al., 2013). However, the high calcium content components of conventional cement

may affect the behavior of Sr and result in behaviors different from other alternative materials (Wieland et al., 2008).

Recently, Ke, et al. (2019) determined the distribution of Sr in a geopolymer with embedded titanate adsorbents at high Sr concentrations. The formation of $SrCO_3$ from high concentrations of Sr was observed to play an important role in immobilizing the Sr inside the waste form generated. That study showed a strong potential for safe storage of Sr in geopolymer waste form even at high Sr concentrations. However, the study does not fully elucidate the behavior at immobilization of low concentrations of Sr, which relates to the actual conditions where radiation dose rates limit the concentration of Sr radioisotopes in intermediate level waste to be low. Additionally, there are no data available for the long-term leaching behavior of Sr from this type of waste, especially considering the contrasting chemical interactions between the titanate adsorbent and geopolymer matrix.

The purpose of this present study is to investigate the leaching behavior and encapsulation mechanisms of Sr in titanate adsorbent embedded in a geopolymer waste form. The titanate adsorbent is loaded with a low concentration of non-radioactive Sr, to replicate the actual conditions in this study. Alkali-activated metakaolin with potassium silicate activator was applied as the waste matrix for encapsulation of the adsorbent. Leaching experiments in deionized water, and a microanalysis of the specimens after different leaching periods, were also conducted.

3.2 Materials and methods

3.2.1 Materials and sorption experiments

The SrTreat® used in the experiments is a commercial hydrous sodium titanate used as a strontium selective ion exchanger (Fortum Power and Heat Oy, Finland). The titanate is a water-insoluble white granular product with a chemical composition $Na_aTi_bO_c \cdot xH_2O$ and grain sizes between 0.3 to 0.85 mm (Figure 3-1). The adsorption process to load Sr^{2+} on the ion exchanger was conducted by exposing the ion exchanger to a non-radioactive 3.3 ppm (37.65 μM) solution of $SrCl_2 \cdot 6H_2O$ (Wako Pure Chemical Industries, Ltd., Osaka, Japan) at a ratio of ion exchanger mass to solution volume of 1:100 (g/mL), and shaking at 160 rpm for 24 hours. Then, the granules were separated by filtration and dried at ambient temperature till achieving a constant weight.

3.2.2 Manufacture of solidified waste form

Alkaline-activated binder components for geopolymer specimens were produced by the reaction between an alkaline activator solution and metakaolin (Metastar® 501, Imerys, UK) as aluminum and silica sources (SiO_2: 51.75 wt.%, Al_2O_3: 43.87 wt.%, and some trace elements). The XRD pattern of the metakaolin is shown in Figure 3-2, the spectrum has a broad peak at around 22° 2θ due to structural disorder of the metakaolin, and peaks from minor crystalline phases anatase, quartz, and mica as impurities. The alkaline activator solution was prepared by dissolving KOH (Wako Pure Chemical Industries, Ltd., Osaka, Japan) pellets into a commercial potassium silicate solution (Wako Pure Chemical Industries, Ltd., Osaka, Japan) to reach a final SiO_2/K_2O molar ratio of solution equal to 1.0, and adding distilled water to give a constant H_2O/K_2O ratio in each sample. The final stoichiometry of the sample is $K_2O{\cdot}Al_2O_3{\cdot}3SiO_2{\cdot}11H_2O$, followed by our previous studies to achieve a dense and stable gel matrix (Duxson et al., 2005), (Ke et al., 2019). The same activator was used for all samples. The mixing process involved mixing the loaded ion exchanger with metakaolin at a mass ratio of 0.30, then adding the prepared alkaline activator solution to form the geopolymer paste. The mixtures were manually blended for 15 minutes using a glass rod and then cast in cylindric 1.3 cm diameter and 1.5 cm high molds, with the lid of each mold tightly sealed by Parafilm. The specimens were cured at 40 °C for 24 hours, followed by 24 hours at 25 °C.

Geopolymer with Sr but with no adsorbent, and conventional cement pastes including Sr with and without adsorbent, were also prepared and used for comparison. For the geopolymer materials without adsorbent, the calculated powder amount of $SrCl_2{\cdot}6H_2O$ was dissolved in water before mixing with the alkaline activator solution, to obtain 2.25 μmol Sr^{2+} in each specimen (assumed as the same calculated amount of Sr^{2+} in the adsorbent including to each geopolymer), then mixed with metakaolin and molded by the same methods as for the geopolymer matrices with adsorbents. Cement paste samples were prepared by mixing the loaded ion exchanger with ordinary Portland cement (standard material “211S” provided by Japan Cement Association) at a mass ratio of 0.30. Then, water was added to give a liquid to solid (OPC and adsorbent) ratio of 0.35. For the cement paste without adsorbent, the calculated powder amount of $SrCl_2{\cdot}6H_2O$ was dissolved in the water before mixing the sample, to obtain 2.25 μmol Sr^{2+} in each specimen. The fresh mixture was

molded and sealed like the geopolymer specimens and cured at ambient temperature for four weeks (Figure 3-3).

3.2.3 Leaching experiments

Leaching experiments were conducted to investigate the leaching behavior of Sr after immersing into deionized water. The ANSI/ANS-16.1-2003 standard test (American Nuclear Society, 2004) was applied. Each specimen was immersed in 88 mL deionized water as leachant (the ratio of leachant volume to specimen surface area is 10 mL/cm^2) as shown in Figure 3-4, and the leachant was completely replaced after cumulative leach times of 2 hours, 7 hours, and 1, 2, 3, 4, 5, 19, 47, 90, 150, 210, 270, 330, and 360 days from the start of the test. Leachate strontium concentrations were determined to measure the released fractions, and solid specimens were removed at 19, 90, and 360 days of leaching time for solid-phase analysis.

3.2.4 Analytical methods

3.2.4.1 Liquid-phase analysis

The solution, after sorption of Sr onto the ion exchanger, and the leachate at each timestep in the leaching experiment was analyzed by inductively coupled plasma-mass spectroscopy (ICP-MS) (iCAP Q ICP-MS, Thermo scientific, USA) (Figure 3-5) to determine the Sr concentration and obtain the leaching rates of Sr from the specimens. Using ICP general-purpose mixed solution (XSTC-331, SPEX CertiPrep, Inc., USA) as a standard solution, and dilute with ultrapure water to a concentration of 0.01, 0.05. 0.1, 0.5, 1.0, 5.0, and 10.0 µg/L for using as a calibration curve. The liquid samples were diluted with ultrapure water, which expected a concentration above the detection limit (0.01 µg/L) and less than 10 µg/L. Each analysis composition was subjected to an acid dilution of 1 vol% in pure nitric acid (Wako Pure Chemical Industries, Ltd., Osaka, Japan) to make a similar background of the measurement samples. The pH values of the liquid samples were also determined by pH meter (D-55, Horiba, Ltd., UK) calibrated by using commercial pH 4.0, 7.0, and 9.0 buffer solutions. The amount of solute adsorbed was calculated using the change between the initial and final dissolved concentrations. Leaching rate calculated by the accumulating concentration of each timestep leaching period, and the initial concentration of Sr in a specimen.

3.2.4.2 Solid-phase analysis

To identify changes in the crystalline phases of the ion exchanger before and after loading with Sr^{2+}, and also in the solidified waste form incorporating Sr^{2+} before and after the leaching, the samples were ground in a mortar and measured by X-ray diffractometry (XRD) (RINT 2000 Rigaku X-Ray Diffractometer, Rigaku, Japan) (Figure 3-6). With Ni filtered Cu-Kα radiation at 30 kV and 20 mA, and a 2θ scan range of 2° to 70° with step size 0.02° and counting time of 1 s/step. The XRD data were processed by Match!3 software (Crystal Impact. Bonn, Germany)

The chemical composition of sectioned polished sample surfaces was observed using scanning electron microscopy (SEM) with energy-dispersive X-ray spectroscopy (EDX) (JSM-IT200, JEOL, Tokyo, Japan) (Figure 3-7), operated at the acceleration voltage of 15 kV, high vacuum mode for mapping. The target elements are Na, Ti, Si, Al, K, Sr. Moreover, using isotope microscope by secondary ion mass spectrometry (SIMS) (CAMECA IMS-1270, CAMECA, France) (Figure 3-8) for detect trace concentrations Sr. For the microscopic imaging, the samples were Pt-coated to increase electric conductivity using an ion sputtering device (JFC-1100E, JEOL, Tokyo, Japan) (Figure 3-9) at a discharge current of 10 mA, with coating time 120 sec. The thin sectioned polished sample surface with Pt-coated is shown in Figure 3-10.

3.3 Results and discussion

3.3.1 Characterization of the titanate adsorbent with Sr

Almost all of Sr^{2+} absorbed by titanate adsorbent. The XRD patterns of the titanate adsorbent before and after loading with Sr^{2+} are shown in Figure 3-11. The titanate adsorbent is identified as a long-range disordered (X-ray amorphous) material, with the broad feature at around 9° 2θ indicating the interlayer spacing of the main edge-sharing TiO_6 sheets (Takahatake et al., 2017), (Ke et al., 2019). With no significant difference in XRD patterns before and after Sr adsorption, this indicates that no new phases have formed, and there are no identifiable crystallographic changes occurring as a result of the adsorption processes.

3.3.2 Leaching rates and distribution of Sr

3.3.2.1 Geopolymer with Sr adsorbed titanate adsorbent

Table 3-1 and Figure 3-12 shows the leaching rate of Sr^{2+} from the geopolymer containing loaded adsorbent. The initial leaching period, within the first 5 days, showed relatively rapid leaching of Sr^{2+}. This situation can be explained as Sr^{2+} wash-out from the superficial parts of the adsorbent particles located near the binder surface, including effects of hydrolysis due to the high selectivity of H^+ on titanate adsorbent (Lehto et al., 1999) according to equation (3-1), when the very alkaline geopolymer was placed into a neutral pH environment.

$$Sr_aTi_bO_c + 2n\ H_2O \rightleftharpoons Sr_{a-n}H_{2n}Ti_bO_c + n\ Sr^{2+} + 2n\ OH^- \quad (3\text{-}1)$$

During the 360 days of the leaching experiment, 0.75% of the Sr^{2+} leached out from the specimen to the leachate (calculated on the basis of the known amount of Sr uptake in the sorbent particles). This shows a high retention performance and limitation by diffusion for Sr^{2+} in the geopolymer matrices with titanate adsorbents, potentially due to the high pH conditions.

The XRD patterns of the K-geopolymer with spent titanate adsorbent before and after leaching are shown in Figure 3-13. The broad hump centered at around 28° 2θ is characteristic of potassium aluminosilicate geopolymer phases (Duxson et al., 2007), (Lizcano et al., 2012), and the small crystalline peaks of anatase and quartz from the metakaolin precursor are also present. Similarly, there is no difference in the patterns between those before and after the leaching for the different periods, indicating that there was no formation of new crystalline products in this experimental system.

The SEM images and elemental maps of the geopolymer specimens with embedded loaded titanate adsorbent Sr before and after leaching for different durations are shown in Figure 3-14. The Ti-rich regions are the adsorbent particles, with the clearly distinguished distribution boundary between adsorbent and matrix, indicating the absence of any interaction that could lead to a breakdown and release of Ti from the titanates between adsorbent and geopolymer matrix during the manufacturing (geopolymerization) and leaching processes. This is consistent with the results of Ke et al. (Ke et al., 2019). There Al- and Si-rich areas consistent with geopolymer regions have no Ti, also indicating no specific interaction. Kuenzel et al. (Kuenzel et al., 2015) observed the interaction between zeolite (clinoptilolite) and geopolymer matrix, and considered that in those

forms, an interfacial alteration zone forming between the zeolite particle and the bulk geopolymer could act as a barrier to aid retention of Cs in the adsorbent. When focusing on Na- and K- rich areas in the results presented here, Na and K were mainly distributed in the titanate adsorbent and the geopolymer matrix before leaching (respectively). However, as the samples age and are leached, the maps show the Na and K distribution becoming indistinct. This indicates that Na in the titanate adsorbent exchanged for K supplied by the geopolymer matrix during the leaching experiment; even though the titanates are not expected to be selective for K^+, the very high concentrations of this ion in the geopolymer pore fluid were sufficient to induce a somewhat high degree of exchange. The Na^+ released from the titanate can be accepted on the negatively charged sites of Al tetrahedra in the geopolymer matrix by a corresponding cation exchange reaction between Na^+ and K^+ during the geopolymerization and leaching processes (Gasca-Tirado et al., 2018).

The low concentration of Sr^{2+} used in this study would be very difficult to detect with SEM-EDX, and so the distribution of Sr alone in the elemental maps were not possible, and Isotope Microscopy (IM) was employed in this study to obtain Sr isotope maps. The IM is a device that uses Secondary Ion Mass Spectrometry (SIMS) technology to provide distribution maps of isotopes in materials and which offers a much lower detection limit than SEM-EDX. The system used here has a spatial resolution of 200 nm in the lateral direction and 10 nm in the depth direction for isotopes up to a concentration of 1 ppb, which is adequate to provide an image of the trace element distribution on the surface of the samples within a small spot size for high precision isotopic imaging (Sakamoto and Yurimoto, 2006), (Sakamoto et al., 2008). Figure 3-15 shows maps of the ^{48}Ti and ^{88}Sr isotopes at selected regions around the center of the geopolymer specimens containing loaded adsorbent before and after leaching. The Ti-rich area indicates the adsorbent particle, and its Sr isotope intensity and distribution remain essentially unchanged even after 360 days of leaching. These isotope maps suggest that almost all of the Sr^{2+} was retained within the titanate adsorbent, although Na^+ was leached out from the adsorbent by cation exchange for K^+ in the matrix. Relate to this, Ke et al. (2019), working at much higher Sr concentrations, concluded that Sr^{2+} was retained inside the titanate adsorbents within their geopolymer matrix samples by the formation of $SrCO_3$ due to oversaturation conditions. However, in this study, no formation of $SrCO_3$ was observed, probably due to the undersaturated conditions. As mentioned above, there is also no chemical barrier formation by interaction and alteration between the adsorbent and matrix. In conclusion, it may be

assumed that Sr^{2+} remained in the titanate particles without formation of a specific low solubility phase or chemical barrier, and despite the extensive cation exchange of Na^{+} for K^{+} entering from the matrix. This retention was presumably achieved due to the higher selectivity of divalent Sr^{2+} than that of the monovalent K^{+} on the adsorption sites of the titanate.

The following sections will show the results of leaching rate and Sr distribution of the other types of specimens. However, some extensive details will discuss in section 3.3.3.

3.3.2.2 Geopolymer-Sr without titanate adsorbent

After 360 days of leaching experiment, 0.05% of Sr leached out from the specimen with very small gradually accumulate leach, as showed in Table 3-2 and Figure 3-16. The XRD patterns showed in Figure 3-17, no different in the patterns between different leaching periods along with the petite peaks of anatase and quartz from the metakaolin precursor. Last, Figure 3-18 shows SEM images and elemental maps of the specimen before leached in deionized water. The elemental maps show the main element as K, Al, Si, which are spread distribution around the geopolymer matrix with no particular distinction was observed. Sr cannot detect because of low concentrations.

3.3.2.3 Ordinary Portland cement with Sr adsorbed titanate adsorbent

The leaching rate of Sr is shown in Table 3-3 and Figure 3-19, 12.23% of Sr^{2+} released from the specimen after 360 days leaching, suggested from the effect of high contents of Ca^{2+} in the system. Figure 3-20 illustrates the XRD patterns, which are similar in all leaching period samples, the crystalline peaks are related to peak of hardened ordinary Portland cement peaks (El-diadamony et al., 2016) with small broad feature at around 9° 2θ from titanate adsorbent layer. Figure 3-21 shows SEM images and elemental maps, Ti-rich areas indicate the adsorbent areas. Ca maps are gradually increase intensity inside the titanate area from the specimen before (Figure 3-21, a), 19 days (Figure 3-21, b), 90 days leached (Figure 3-21, c), and obviously in 360 days leached (Figure 3-21, d), reversible with Na maps intensity which has high intensity on the matrix area after long time leached, indicated the high efficiency of Ca^{2+} to exchange with Na^{+} and Sr^{2+} on titanate layered.

3.3.2.4 Ordinary Portland cement-Sr without titanate adsorbent

The high leaching rate of 50.63% of Sr^{2+} leached out from specimen after 360 days leaching (Table 3-4 and Figure 3-22) because of the effect of Ca^{2+} in the system. The XRD patterns (Figure 3-23) mainly show hardened OPC crystalline peaks with no different peaks among the different leaching periods. SEM images and elemental maps of the specimen before leached in deionized water, as shown in Figure 3-24, displays main impurity elements (Ca, Si, Al, Mg, S, Fe) distribute in the matrix of a specimen with no peculiar evident.

3.3.3 Comparison of retention efficiency of the waste forms with Sr

To compare the efficiencies of the retention of Sr^{2+} inside the geopolymer matrix, specimens of K-geopolymer without titanate adsorbent and specimens of ordinary Portland cement (OPC) with and without titanate adsorbent were also investigated (Figure 3-25). Even without the addition of the titanate adsorbent, almost all of the Sr^{2+} was retained in the geopolymer matrix, indicating that the geopolymer matrix itself offers a high potential to immobilize Sr^{2+} in case it is released from a loaded exchanger particle (Figure 3-25, curve a). Only 0.05 % of the Sr^{2+} leached out from the matrix after 360 days of leaching. At the low concentration of Sr^{2+}, the Sr^{2+} ions are easily accommodated within the geopolymer gel framework and do not significantly change the local gel structure (Walkley et al., 2020). This indicates that both the titanate adsorbent in K-geopolymer matrix and the K-geopolymer itself offers a high potential for Sr immobilization.

The leaching ratios of OPC with titanate adsorbent (12.23 % after 360 days in Figure 3-25, curve c) and without titanate adsorbent (50.63% after 360 days in Figure 3-25, curve d) were very much higher than those the of geopolymer, however. With the adsorbent, Sr^{2+} in the adsorbent may leach out to the matrix by cation exchange with Ca^{2+} in the pore solution of the OPC matrix. With the similar properties of Sr^{2+} and Ca^{2+}, the selectivity of Sr^{2+} and Ca^{2+} on the layered titanate structure is not significantly different (Lehto and Clearfield, 1987), (Lehto et al., 1999). In the initial stage of the leaching experiment, the exchange process may proceed due to the steeper activity gradient of Sr^{2+} and Ca^{2+} between the adsorbent and the OPC matrix. After the Sr^{2+} is leached or exchanged from the adsorbent into the cement binder, Sr^{2+} shows a lower preference than Ca^{2+} for substituting and binding with hydrated phases in cements when in contact with alkaline pore fluid (Atkins and Glasser, 1992). For this reason, the OPC matrix has a poor ability to prevent the release of Sr^{2+},

which has moved into the OPC matrix. Eventually, much of Sr^{2+} is leached from the OPC specimens, as shown in the experimental results.

Finally, the encapsulation mechanisms of the low concentration Sr in the titanate adsorbent within a K-geopolymer matrix is summarized (Figure 3-26). The K-geopolymer matrix provides favorable chemical conditions for immobilization of Sr^{2+} in the adsorbent. First, the K-geopolymer imposes hyperalkaline conditions which are able to completely reduce exchanges by H^+. The H^+ has the highest selectivity among several cations in the following order: $H^+ >> (Sr^{2+} \approx Ca^{2+}) >> K^+ > Na^+$ (Lehto et al., 1999). This suggests that in a hyperalkaline system, the exchange of Sr^{2+} for H^+ is very highly restricted because of the low activity of H^+ (Figure 3-26, b). Second, the K-geopolymer matrix also provides a high-K environment surrounding the adsorbent. Due to the higher cation exchange selectivity of Sr^{2+} over K^+, Sr cations are selectively retained in the adsorbent (Figure 3-26, a), although Sr cations would easily be leached out from the adsorbent in a high Ca system such as in an OPC matrix. However, in the high pH and K conditions such as our matrix, the interference by external Ca is not detrimentally affected the Sr exchange because competitive calcium concentration is limited at high pH conditions due to precipitation hydroxide and/or carbonate. Third, metakaolin-based geopolymer provides the sites with a negative charge in the Al-tetrahedra enabling Sr retention, even if it could be released from the titanate particles. The Sr^{2+} cations are easily accommodated within a geopolymer gel framework at low concentrations, and do not significantly change the local gel structure (Walkley et al., 2020) (Figure 3-26, c). On this reasoning, this study clearly suggests that a geopolymer structure formed by K-silicate activation of metakaolin offers an excellent form for a waste matrix that limits Sr leaching from loaded titanate adsorbent granules.

3.4 Conclusions

Titanate adsorbents exhibited high selectivity for Sr^{2+} and maintained their initial physical and chemical properties during embedding (in particulate form) in geopolymer binders, and through the subsequent leaching processes. After encapsulation of the adsorbent with a realistic Sr concentration in a K-silicate-activated metakaolin-based geopolymer, almost all of the Sr was retained in the adsorbent without formation of precipitating phases or interfacial alterations between the titanate and geopolymer. A low leaching rate of Sr (0.75 % released after 360 days of leaching) arises from the hyperalkaline geopolymer pore fluid conditions which limit the Sr^{2+}

exchange by H^+, the high K content of the system further limits leaching out of Sr, and there are sites that strongly fix Sr by ion-exchange onto the geopolymer framework in the event that it is released by the titanate. In addition to other advantages of geopolymer materials such as the excellent thermal resistance, the potential of designs for a relatively low content of free water, and prevention of hydrogen release with its attendant danger of explosion, the low leaching rate of Sr suggests the K-aluminosilicate geopolymer is an excellent candidate for a waste matrix in a form that is suitable for long term storage and disposal of spent titanate adsorbent in the proper repository.

Figure 3-1 SrTreat® as received and its powder

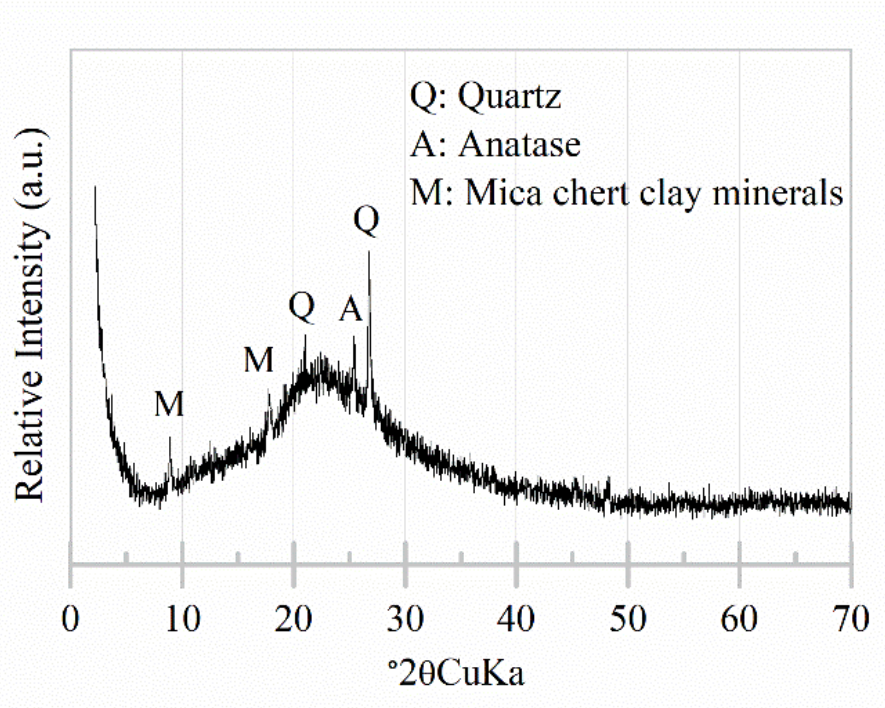

Figure 3-2 XRD pattern of the metakaolin precursor

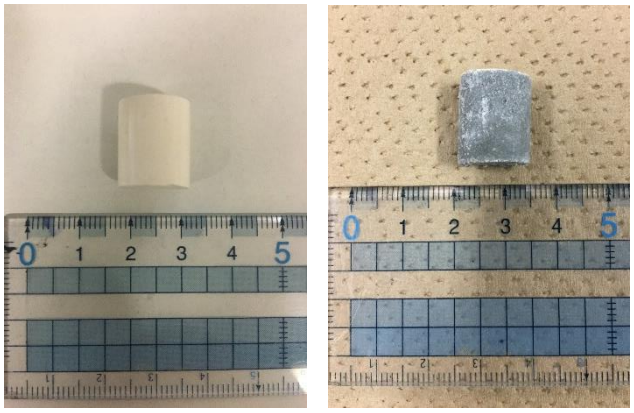

Figure 3-3 Geopolymer (left) and Cement (right) specimen

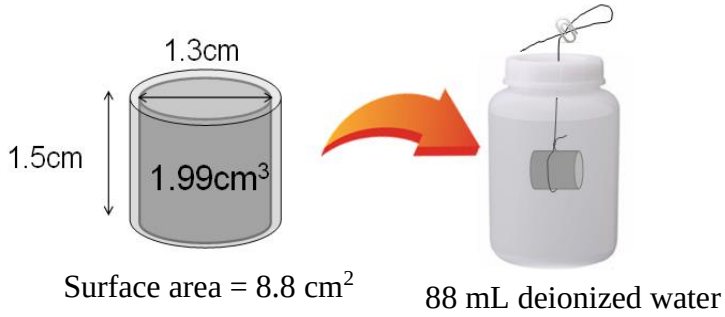

Figure 3-4 Schematic of leaching experiments

Figure 3-5 Inductively coupled plasma-mass spectrometry (ICP-MS)

Figure 3-6 X-Ray Diffractometer (XRD)

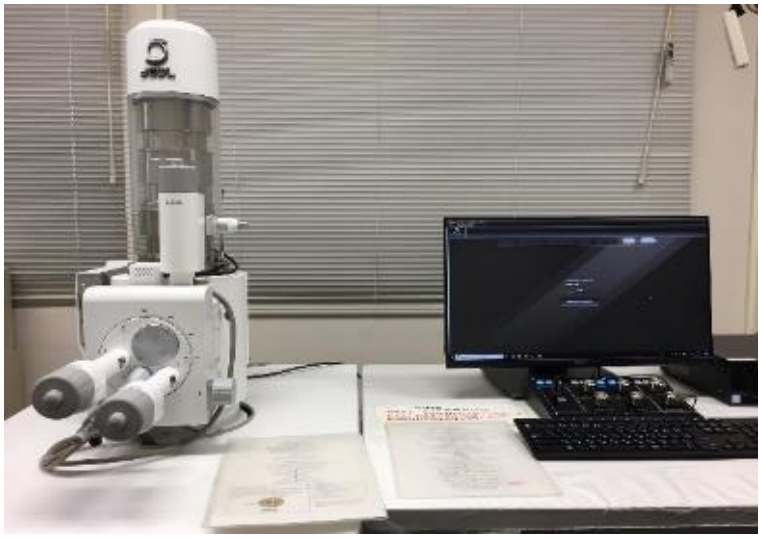

Figure 3-7 Scanning Electron Microscopy (SEM)

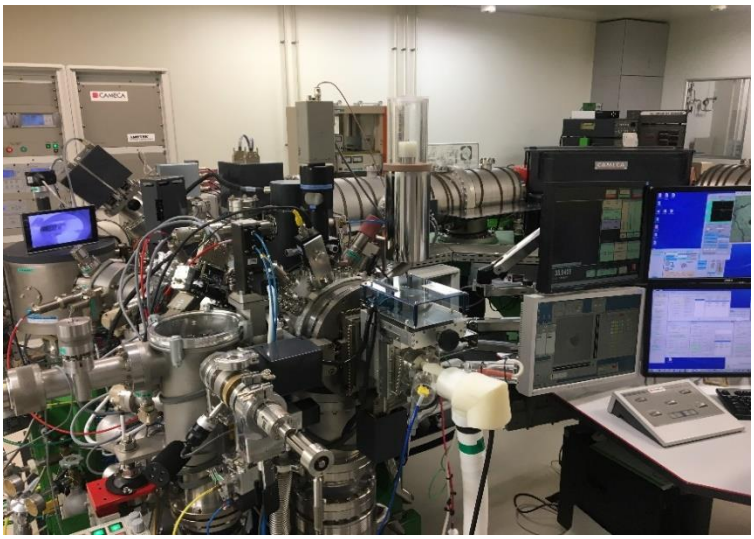

Figure 3-8 Secondary ion mass spectrometry (SIMS)

Figure 3-9 Ion sputtering device

Figure 3-10 Thin sectioned polished sample surfaces with Pt coating

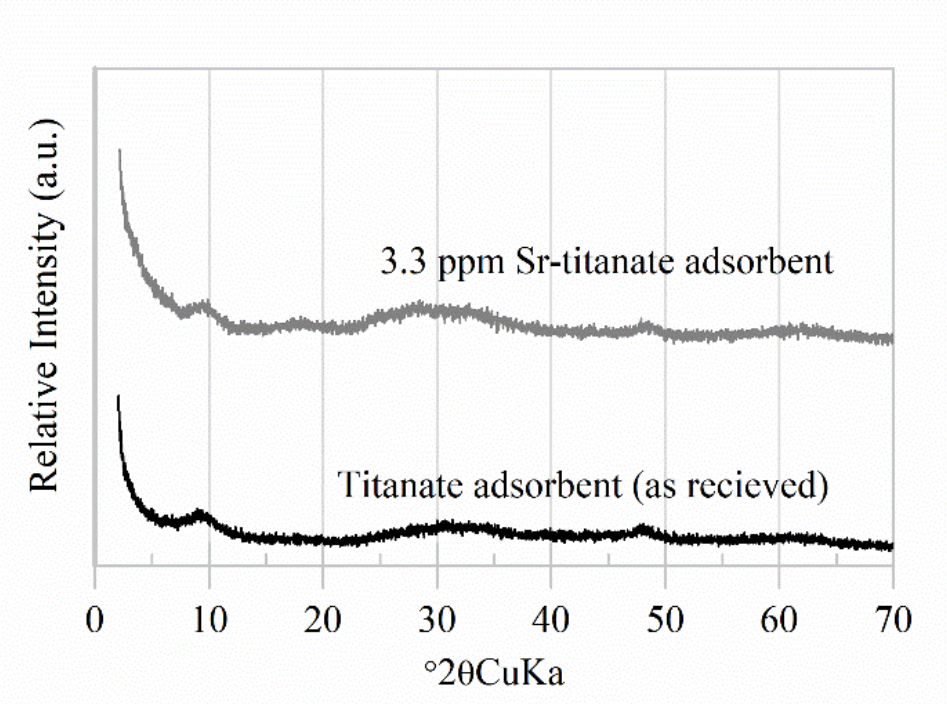

Figure 3-11 XRD patterns of titanate adsorbent before and after loading with Sr^{2+}

Table 3-1 Cumulative leaching of Sr^{2+} from geopolymer with titanate adsorbent from each leach time

Leach time (days)	Cumulative leached rate (%)
0.083 (2 hours)	0.04
0.292 (7 hours)	0.09
1	0.15
2	0.25
3	0.30
4	0.35
5	0.43
19	0.53
47	0.55
90	0.58
150	0.62
210	0.67
270	0.71
330	0.74
360	0.75

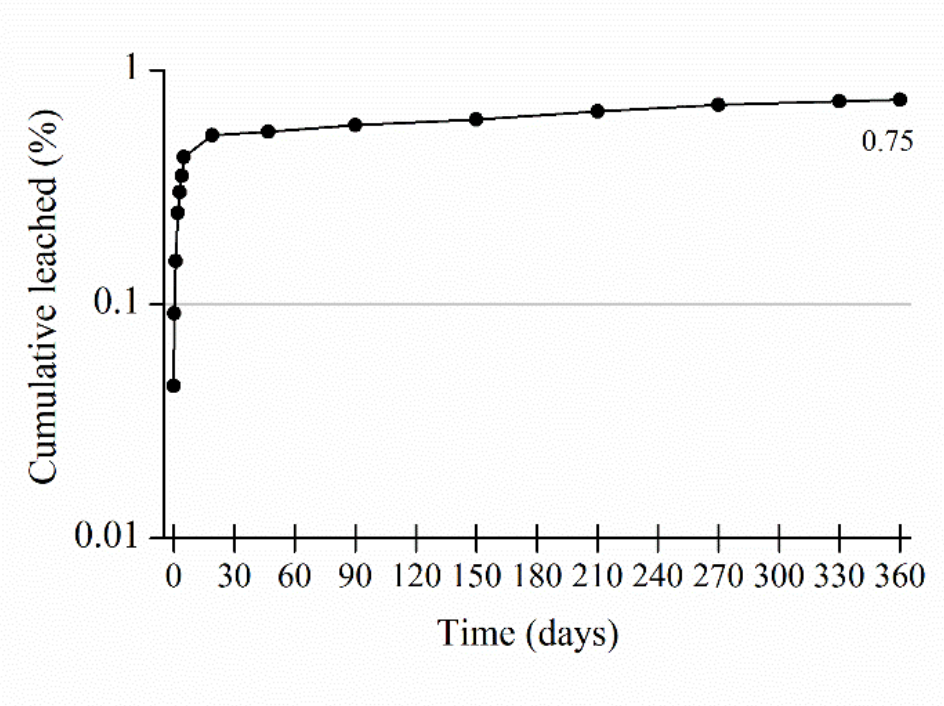

Figure 3-12 Cumulative leaching of Sr^{2+} from geopolymer mixed with titanate adsorbent, applying the ANSI/ANS 16.1 test method with full replacement of leachate at each sampling point shown

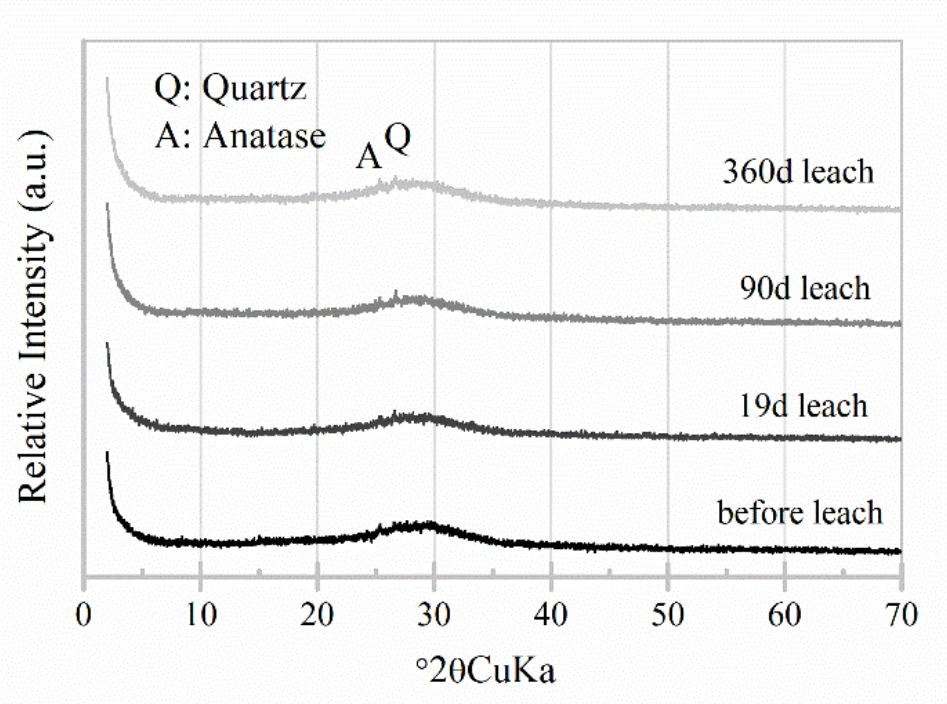

Figure 3-13 XRD patterns of K-geopolymer with spent titanate adsorbent loaded Sr before and after leaching for different durations as marked

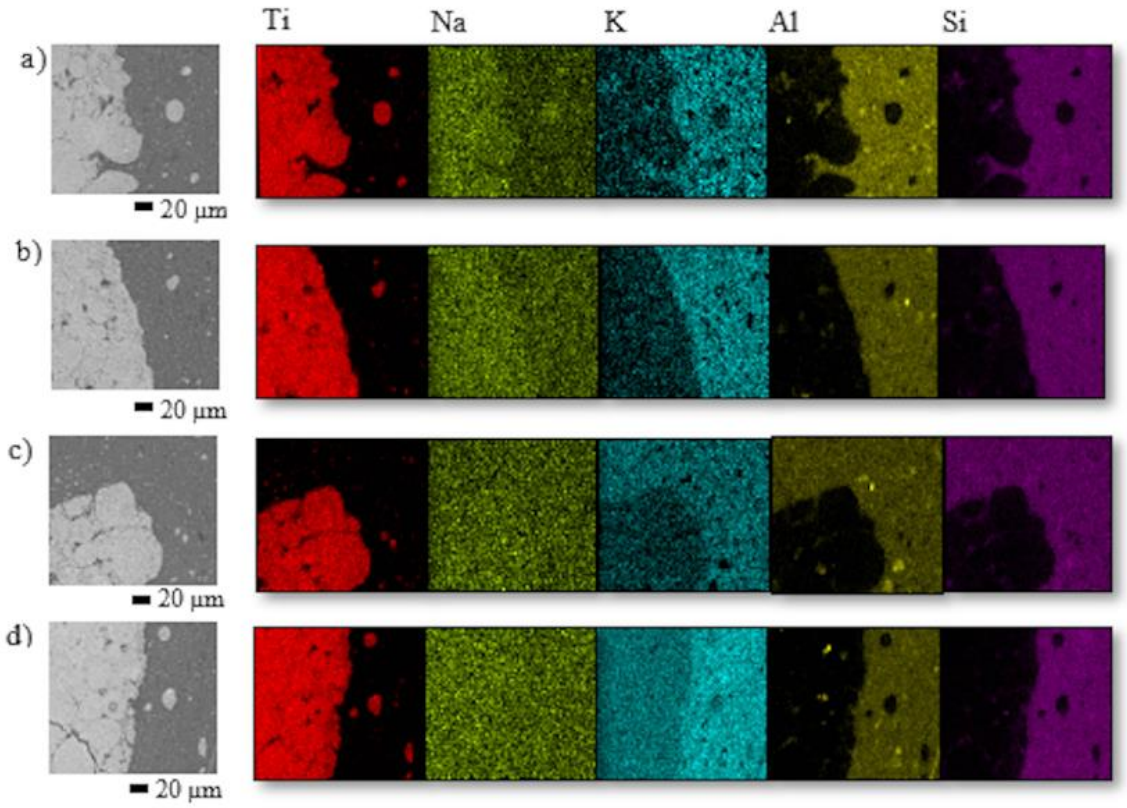

Figure 3-14 SEM images and elemental maps of geopolymer specimens with titanate adsorbent loaded Sr; a) before, and after b) 19days, c) 90days, and d) 360 days of leaching in deionized water

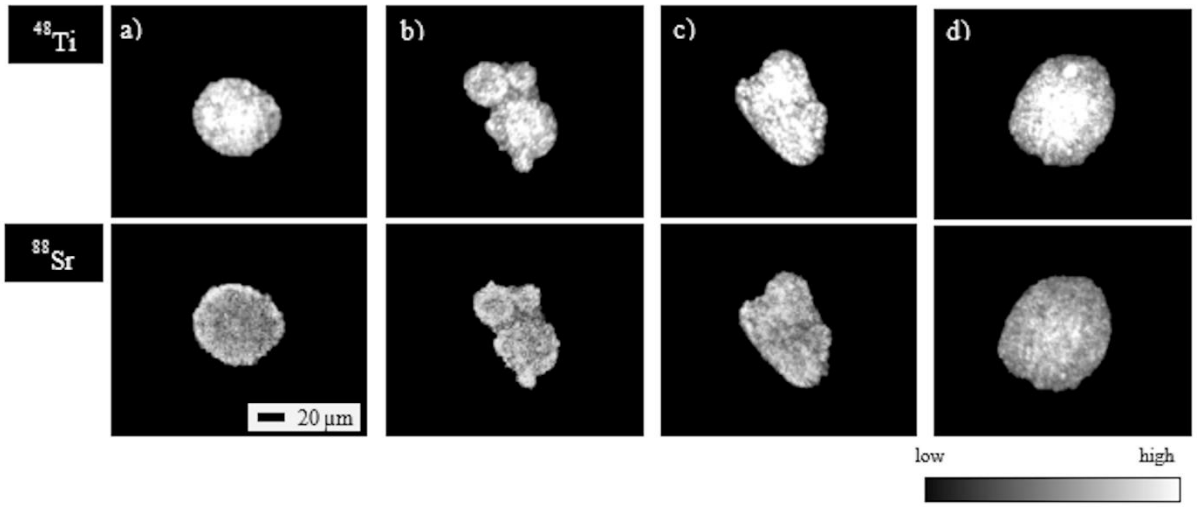

Figure 3-15 ^{48}Ti and ^{88}Sr isotope maps surrounding a titanate adsorbent particle in geopolymer specimens a) before, and after b) 19 days, c) 90 days, and d) 360 days of leaching in deionized water

Table 3-2 Cumulative leaching of Sr^{2+} from geopolymer without titanate adsorbent from each leach time

Leach time (days)	Cumulative leached rate (%)
0.083 (2 hours)	0.00
0.292 (7 hours)	0.01
1	0.01
2	0.01
3	0.01
4	0.01
5	0.01
19	0.02
47	0.02
90	0.02
150	0.03
210	0.03
270	0.04
330	0.04
360	0.05

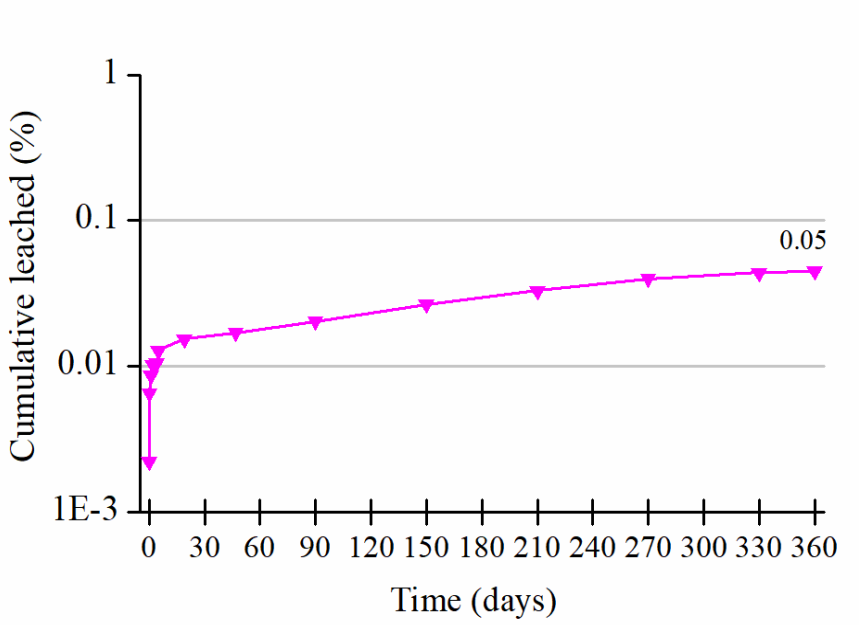

Figure 3-16 Cumulative leaching of Sr^{2+} from geopolymer without titanate adsorbent

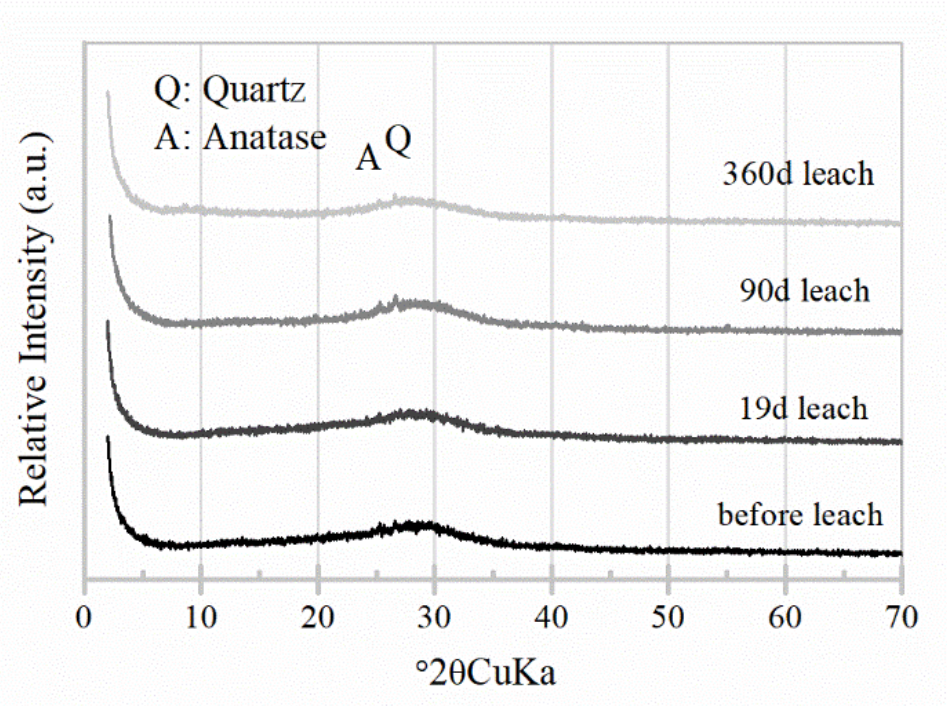

Figure 3-17 XRD patterns of K-geopolymer loaded Sr without spent titanate adsorbent before and after leaching for different durations as marked

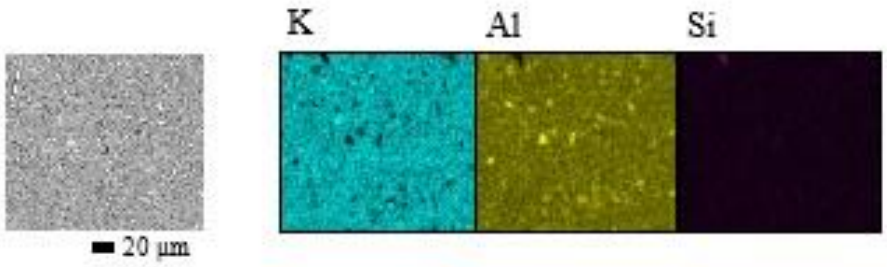

Figure 3-18 SEM images and elemental maps of geopolymer specimens loaded Sr without titanate adsorbent before leaching in deionized water

Table 3-3 Cumulative leaching of Sr^{2+} from ordinary Portland cement with titanate adsorbent from each leach time

Leach time (days)	Cumulative leached rate (%)
0.083 (2 hours)	0.08
0.292 (7 hours)	0.32
1	0.97
2	1.70
3	2.38
4	3.05
5	3.74
19	6.39
47	7.56
90	8.15
150	8.84
210	9.69
270	10.48
330	11.51
360	12.23

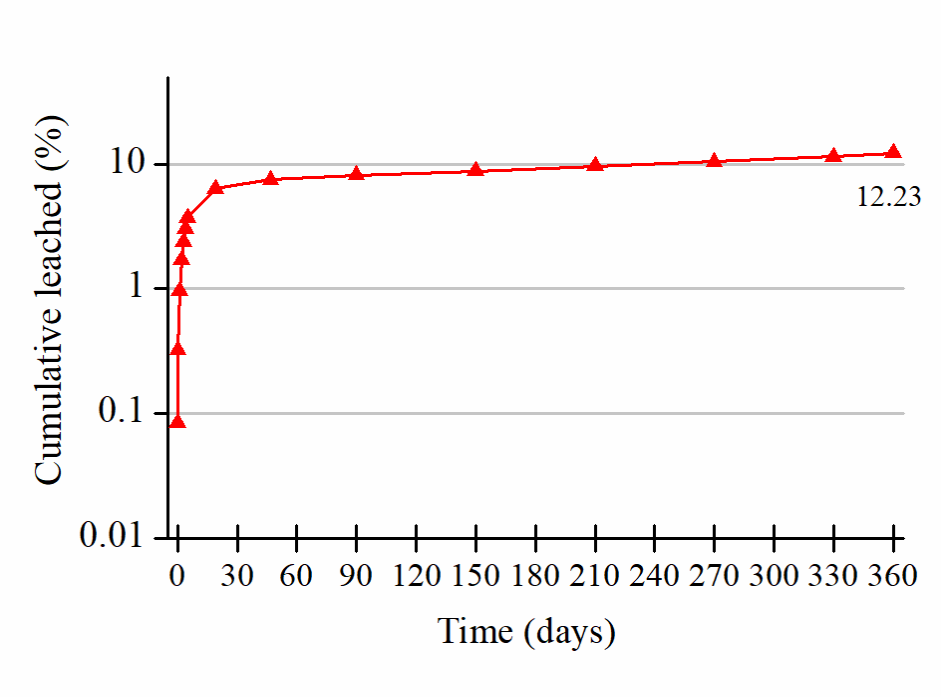

Figure 3-19 Cumulative leaching of Sr^{2+} from ordinary Portland cement with titanate adsorbent

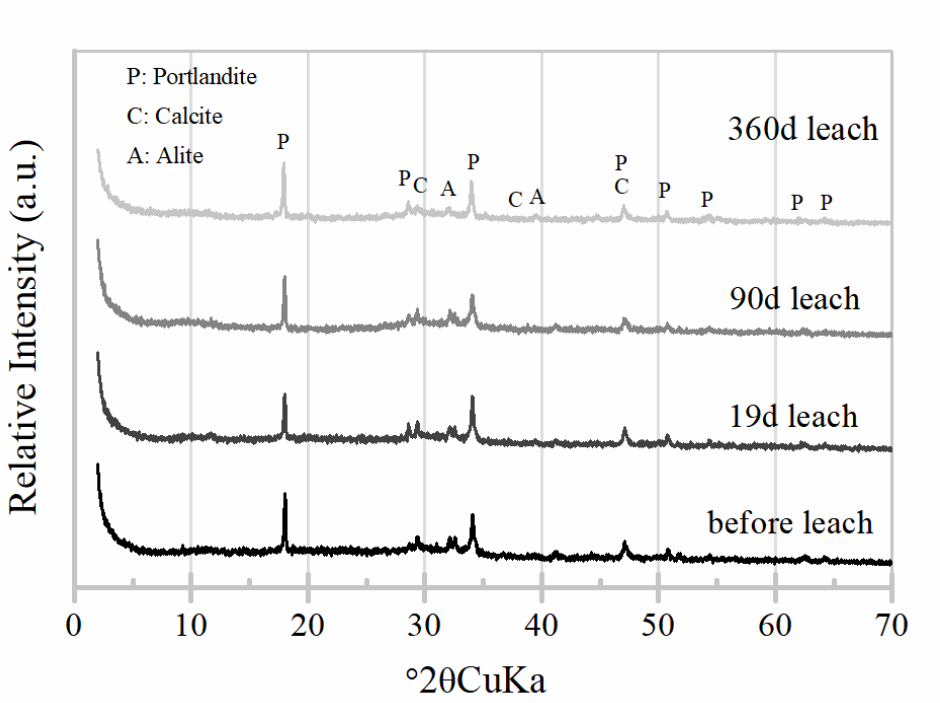

Figure 3-20 XRD patterns of ordinary Portland cement with spent titanate adsorbent loaded Sr before and after leaching for different durations as marked

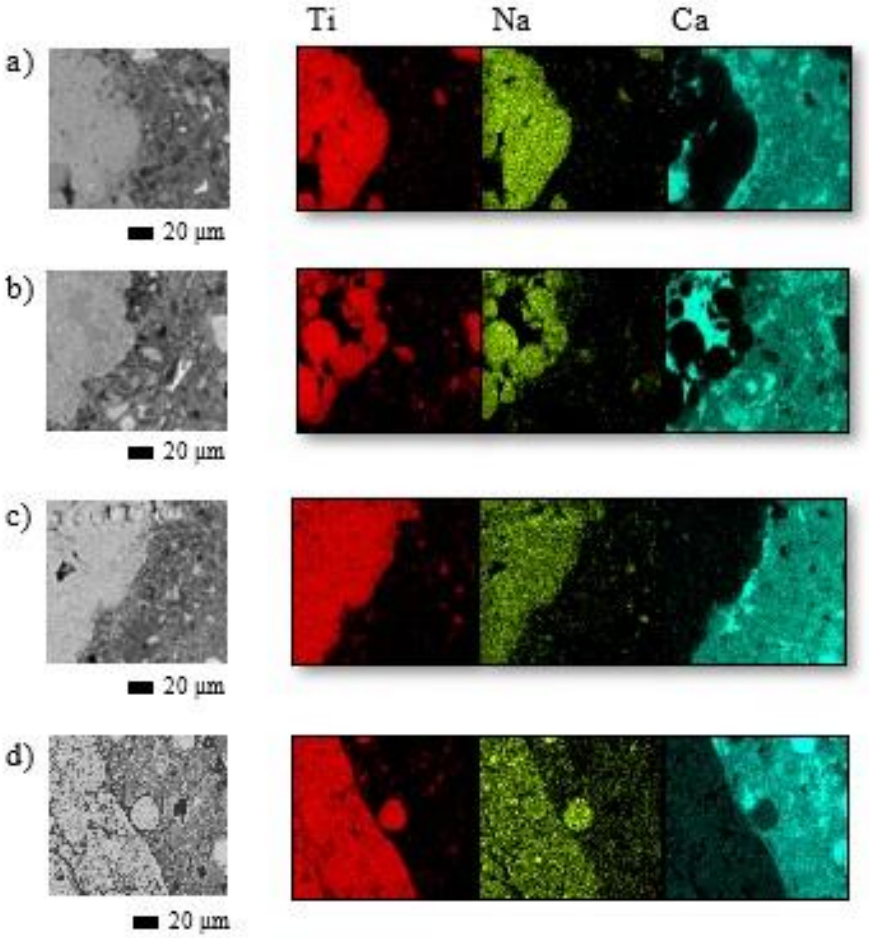

Figure 3-21 SEM images and elemental maps of ordinary Portland cement specimens with titanate adsorbent loaded Sr; a) before, and after b) 19days, c) 90days, and d) 360 days of leaching in deionized water

Table 3-4 Cumulative leaching of Sr^{2+} from ordinary Portland cement without titanate adsorbent from each leach time

Leach time (days)	Cumulative leached rate (%)
0.083 (2 hours)	0.38
0.292 (7 hours)	1.46
1	4.08
2	6.73
3	8.95
4	10.96
5	12.78
19	21.62
47	27.24
90	33.10
150	37.79
210	40.90
270	44.18
330	48.61
360	50.63

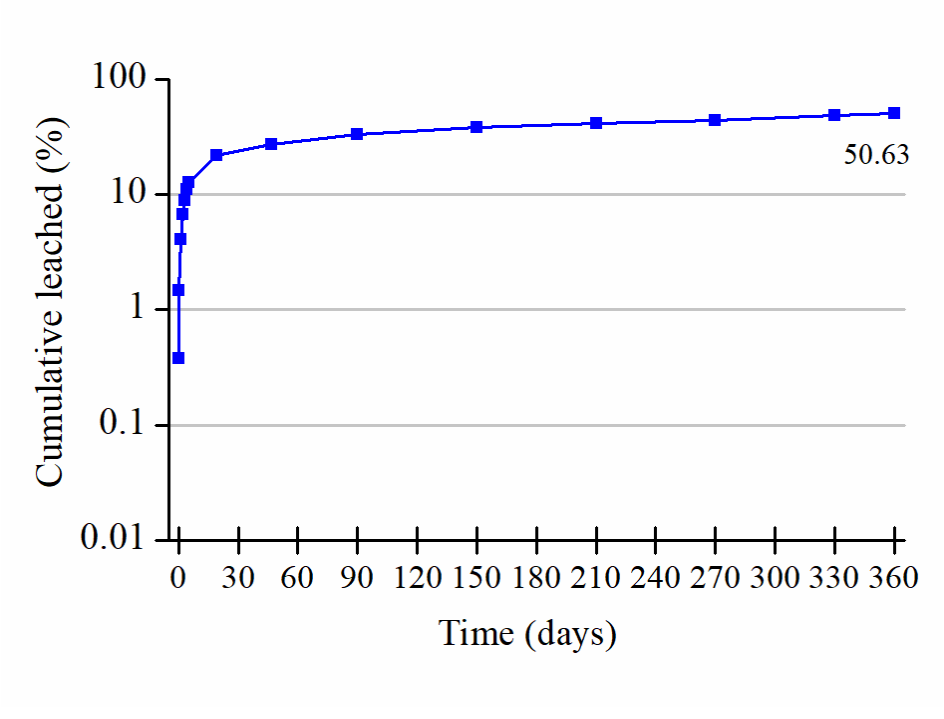

Figure 3-22 Cumulative leaching of Sr^{2+} from ordinary Portland cement without titanate adsorbent

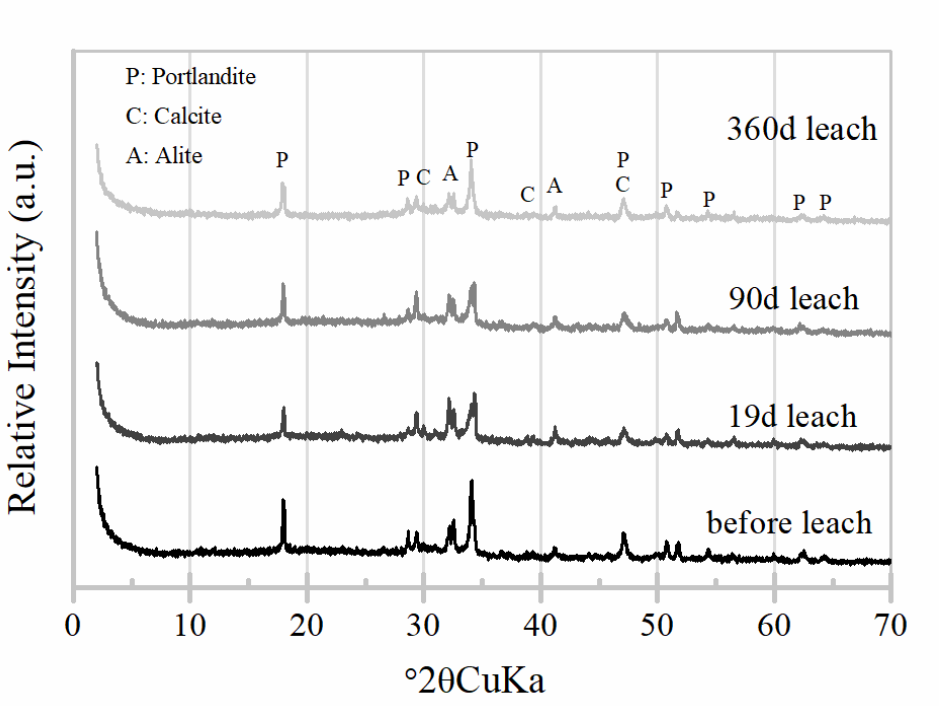

Figure 3-23 XRD patterns of ordinary Portland cement loaded Sr without spent titanate adsorbent before and after leaching for different durations as marked

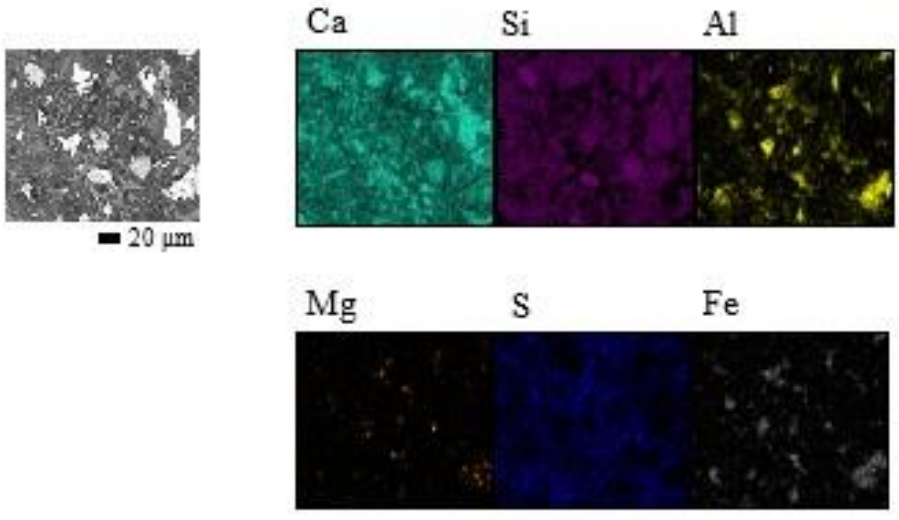

Figure 3-24 SEM images and elemental maps of ordinary Portland cement specimens loaded Sr without titanate adsorbent before leaching in deionized water

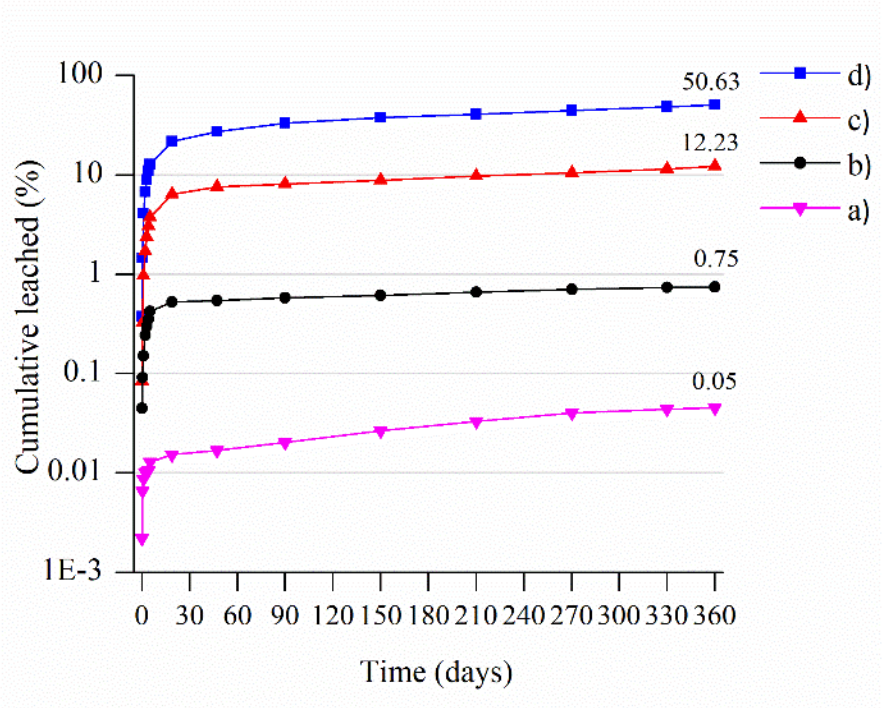

Figure 3-25 Cumulative leached percentage of Sr^{2+} from: a) geopolymer without adsorbent, b) geopolymer with adsorbent, c) cement with adsorbent, d) cement without adsorbent

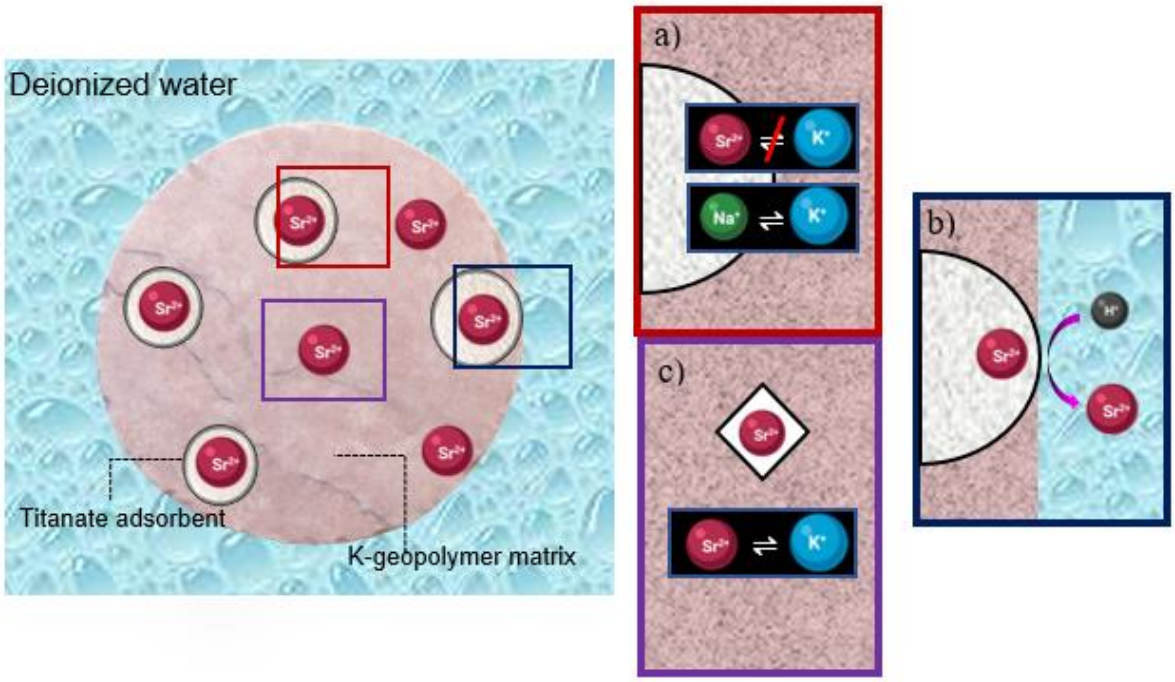

Figure 3-26 Schematic diagram of geopolymer matrix encapsulated titanate adsorbent adsorbed strontium, the interaction where a) between titanate adsorbent and geopolymer matrix inside specimen, b) the edge between titanate adsorbent and deionized water, c) geopolymer binder area

Chapter 4: Encapsulation of Cs-loaded titanate spent adsorbent in Potassium Aluminosilicate geopolymer

4.1 Introduction

In the previous chapter, the mechanism of Sr in titanate adsorbent embed in the geopolymer waste form was discussed. On the other hand, the primary radioactive elements from the nuclear reactor accidental, such as Cs which is still remain and unusual in the trial for adsorbed by titanate adsorbent and should be investigated the optional ways for encapsulation of these Cs radionuclides.

As well known, titanate adsorbent showed the possibly efficiency to exchange the other cations with Na^+ at the interlayer space of the layered titanate structure. Focusing on Cs cation, there have some studies about the incorporation of Cs with titanate adsorbent, e.g., the synthetic layered cesium titanate used for photocatalytic production (Pilarski et al., 2018), and the host materials for safe disposal of high-level radioactive waste (Grey et al., 1985). Following this, the proper conditioning for solidification waste towards the safety requirements and reduce the radionuclides leach rates are required.

Radioactive wastes in the disposal facility are crucial to prevent the migration and dispersion of radionuclides to the environment. The wastes must be non-dispersible, insoluble, and good mechanical and structural ability. Many studies investigated the alternative monolithic solidified product for Cs immobilization, for example, fly ash belite cement (Goni et al., 2006), alkaline activated fly ash matrix (Fernández-Jiménez et al., 2005) and zeolite (El-Kamash et al., 2006) was proposed and classified as good solidify systems for Cs. The superior Cs^+ retention of alkaline-activated materials (Shi and Fernández-Jiménez, 2006) concluded much less interference with hydration of alkaline-activated materials than ordinary Portland cement waste (Blackford et al., 2007). On the other hand, the solidified conventional cementitious materials have high leachability of radionuclides, especially to Cs, the sorption of Cs in the cement matrix is low, and Cs also remains soluble in the high pH environment of cement (Plecas et al., 1992). Thus, the kind of materials with low content on calcium is preferably needed.

Even though numerous amounts of studies on immobilizing Cs^+ on different systems have been proposed, however, the immobilization mechanisms of Cs on titanate adsorbent embedded K-

aluminosilicate geopolymer is very lacking information. In this study, the aim was to present the alternative way to absorb Cs and investigate the possibility of solidifying titanate adsorbent loaded with Cs, in K-based geopolymer waste form. The leaching characteristics and encapsulation mechanisms of Cs have been studied. The titanate adsorbent is loaded with a low concentration of non-radioactive Cs, to replicate the actual conditions. Alkali-activated metakaolin with a potassium silicate activator was investigated as the waste matrix for the embedment of the adsorbent. Leaching experiments in deionized water, and microanalysis of the specimens after different leaching periods, were also conducted for this purpose.

4.2 Materials and methods

4.2.1 Materials and sorption experiments

The adsorption process to load Cs^+ on the commercial sodium titanate ion-exchanger SrTreat® (Fortum Power and Heat Oy, Finland) was conducted by contacting the ion exchanger and 10 ppm Cesium Standard Solution (Wako Pure Chemical Industries, Ltd., Osaka, Japan) at a solid/liquid ratio of 1:100 (g/mL), according to the recommendation by the Japan Atomic Energy Society immediately after the accident (Saito et al., 2018), shaking at 160 rpm for 24 hours. Then, the powder was separated by filtration and dried at ambient temperature till reaching a constant weight. The solution after sorption was analyzed by inductively coupled plasma-mass spectroscopy (ICP-MS) (iCAP Q ICP-MS, Thermo scientific, USA) to calculate the amount of cesium loading in titanate adsorbent.

4.2.2 Manufacture of solidified waste form

Metakaolin (Metastar® 501, Imerys, UK) was used to synthesize binder with chemical composition as SiO_2: 51.75 wt.%, Al_2O_3: 43.87 wt.%, and some trace elements. Activating solutions were produced using potassium silicate solution (Wako Pure Chemical Industries, Ltd., Osaka, Japan), KOH pellets (Wako Pure Chemical Industries, Ltd., Osaka, Japan), and deionized water to reach the final stoichiometry of sample $K_2O{\cdot}Al_2O_3{\cdot}3SiO_2{\cdot}11H_2O$ (according to previously studied to achieve dense and stable of gel matrix (Duxson et al., 2005), (Ke et al., 2019)). The mixing process was prepared by mixing the adsorbed ion exchanger with metakaolin in the mass ratio of 0.3, then adding the prepared alkaline activator solution to form the geopolymer paste. The mixtures were manually blended for 15 minutes to give homogenization and put in cylindrical shape mold with

1.3 cm diameter and 1.5 cm height, with the lid of each mold sealed by Parafilm and vibrated to remove air bubbles. After that, cured the specimens at 40°c for 24 hours and 25°c for 24 hours.

Geopolymer incorporating Cs, and conventional cement pastes, including Cs with and without adsorbent, were also prepared and used for comparison. The calculated powder amount of CsCl (Wako Pure Chemical Industries, Ltd., Osaka, Japan) was dissolved and mixed with alkaline activator solution, to obtain 4.25 μmol Cs^+ in each specimen (assumed as the same amount of Cs^+ in the adsorbent combining in each geopolymer), then mixed with metakaolin and molded by the same methods as for the geopolymer matrices with adsorbents. Cement past was simulated by mixing loaded adsorbent with ordinary Portland cement (standard material "211S" provided by Japan Cement Association) at a mass ratio of 0.30. After, water was added to give a liquid to solid (OPC and adsorbent) ratio of 0.35. For the cement paste without the adsorbent, the powder amount of CsCl was dissolved in the water before mixing the sample, to obtain 4.25 μmol Sr^{2+} in each specimen. The lid of the 1.3 cm diameter and 1.5 cm height cylindrical shape mold was tightly closed after the fresh mixture was poured and cured at ambient temperature for four weeks.

4.2.3 Leaching experiments

Leaching of Cs from the samples was determined using the ANSI/ANS-16.1-2003 standard test (American Nuclear Society, 2004). Dried specimens were de-molded and immersed in 88 mL deionized water as leachant, and the leachant was replaced after cumulative leach times of 2 hours, 7 hours, and 1, 2, 3, 4, 5, 19, 47, 90, 150, 210, 270, 330, and 360 days from the start of the test. Leachate cesium concentrations were determined to measure the released fractions, and solid specimens were removed at 19, 90, and 360 days of leaching time for solid-phase analysis. The solutions were analyzed by inductively coupled plasma-mass spectroscopy (ICP-MS) (iCAP Q ICP-MS, Thermo scientific, USA) for determining the Cs concentration to obtain the leaching rates of cesium from the specimens.

4.2.4 Analytical methods

Changes in the crystalline structure of adsorbent before and after Cs incorporation, also the waste form before and after leaching was assessed using the X-ray diffractometry (XRD) (RINT 2000 Rigaku X-Ray Diffractometer, Rigaku, Japan) with Cu-Kα radiation at 30 kV and 20 mA, the 2θ scan range of 2° to 70°. The chemical composition of sectioned polished sample surface was observed using scanning electron microscopy (SEM) with energy-dispersive X-ray spectroscopy

(EDX) (JSM-IT200, JEOL, Tokyo, Japan), operated at the acceleration voltage of 15 kV, and field emission electron probe microscope (FE-EPMA) (JXA-8350F, JEOL, Tokyo, Japan) (Figure 4-1). The EPMA is equipped with wavelength dispersive spectrometer (WDS), and the measurement conditions consisted of an acceleration voltage of 15 kV, the unit measurement time of 10 ms/point, a pixel size of 985 μm x 6405 μm with interval 5 μm x 5 μm. For the microscopic imaging, the samples were Pt-coated to increase electric conductivity using an ion sputtering device (JFC-1100E, JEOL, Tokyo, Japan) at a discharge current of 10 mA, with coating time 120 sec.

4.3 Results and discussion

4.3.1 Characterization of the titanate adsorbent with Cs

Figure 4-2 shows the XRD patterns of titanate adsorbent before and after adsorbing with Cs^+, similarly with the titanate adsorbent adsorbing with Sr^{2+}, the amorphous material with broad hump around 9° 2θ. Underlining the titanate adsorbent is a stable material with no significant difference, no degradation, and no new phase formed after Cs adsorption.

4.3.2 Leaching rates and distribution of Cs

4.3.2.1 Geopolymer with Cs adsorbed titanate adsorbent

The leaching rate of Cs^+ from the matrix loading adsorbent is shown in Table 4-1 and Figure 4-3, The early leaching period also showed initial fast leaching of Cs^+ from the adsorbent particle superficial surface of the specimen, including hydrolysis effects due to the high selectivity of H^+ on titanate adsorbent as expressed in equation 4-1.

$$Cs_aTi_bO_c + n\ H_2O \rightleftharpoons Cs_{a-n}H_nTi_bO_c + n\ Cs^+ + n\ OH^- \quad (4\text{-}1)$$

Within 360 days of the leaching experiment, 6.92% of the Cs^+ leached out from the specimen to the leachate. It shows slightly high retention performance for Cs^+ in the geopolymer matrices loading titanate adsorbent.

The XRD patterns of K-geopolymer with spent titanate adsorbent before and after leached (Figure 4-4). The amorphous structure of the geopolymer matrix with tiny crystalline peaks of anatase and quartz from the metakaolin precursor was observed. The broad non-crystalline hump center at around 28° 2θ, is characteristic of potassium alumino-silicate phase (Duxson et al., 2007).

Similarly, no peaks different crystalline intrusion of specimens between before leached and specific leached period.

The SEM images and elemental maps of the specimens embedded titanate adsorbent loaded Cs before and after leaching with different periods are shown in Figure 4-5. The Ti-rich regions express the adsorbent with the detected distribution boundary between adsorbent and matrix, indicating no specific interaction occurred between adsorbent and geopolymer matrix during manufacturing (geopolymerization) and leaching processes. There Al- and Si-rich areas consistent with the geopolymer region's absence of Ti, also indicating no specific interaction and remain a few spots of nonreactive materials. Following this, focusing on Na- and K- rich areas, Na and K was mainly allocated in titanate adsorbent and geopolymer matrix before leaching, respectively. Though, as a leaching time pass, the similar gradient on both Na and K maps becomes. As aforementioned, Na can exchange with K on titanate adsorbent during the leaching period. Also, Na^+ from titanate adsorption can be accepted on the negatively charged sites of Al tetrahedron in the geopolymer matrix by a cation exchange reaction between Na^+ and K^+ during the geopolymerization and leaching processes.

The compositional mapping by EPMA showed the intensity of the elements (Figure 4-6). Ti, Al, Si distributions support the information to clarify the adsorbent particle and geopolymer matrix regions with unchanged relative concentrations in the specific area of samples between before and after leaching processes. Compared of each elemental map before leached (Figure 4-6, a) with 19 days (Figure 4-6, b), 90 days (Figure 4-6, c) and 360 days (Figure 4-6, d) leached, Na concentration in the titanate particle reduces after long time leaching and seems to be the same intensity on the whole measuring area. About K intensity, which is dominant in the matrix field and obviously differs from the intensity on titanate part at 0-day leaching, after 360 days leaching that the intensity becomes practically similar intensity above the total area. Na^+ and K^+ behaviors will act as the same as the discussion of the matrix with Sr loaded adsorbent. Aim attention at Cs distribution shows Cs concentrations are abundant in the titanate adsorbent before leaching and continually decrease after leaching processes. Consistence with the Cs leaching rate and suggested that Cs^+ and K^+ can exchange each other. On the titanate adsorbent, a few Cs^+ can possibly replace by K^+ from the very high concentrations of this ion in the geopolymer pore fluid as the radii size of K^+ are smaller than Cs^+. However, the exchange of Cs^+ and K^+ is limited because the collapsed

structure that occurred from the Cs adsorption process may lead to the potential of cation irreversible. Also, The Cs^+ released from the titanate can be substituted with K^+ and Na^+ on the negatively charged sites on the geopolymer matrix during the geopolymerization and leaching processes.

The following sections will show the results of the leaching rate and Cs distribution of the other types of specimens. However, the extensive details will discuss in section 4.3.3.

4.3.2.2 Geopolymer-Cs without titanate adsorbent

After 360 leaching days, 11.38% of Cs^+ released out with the moderately increase leach, as shown in Table 4-2 and Figure 4-7. The XRD pattern also underlined no difference in the patterns between different leaching periods (Figure 4-8). EPMA elemental maps showed the major elements on geopolymer loaded Cs without titanate adsorbent (Figure 4-9). Comparison, the elemental map of each element, distributes among before leached (Figure 4-9, a),19 days (Figure 4-9, b), 90 days (Figure 4-9, c) and 360 days (Figure 4-9, d) leached, Cs and K, which are act as charge balance on the geopolymer framework, reduce over the increase leaching time. K is concentrating on the system and dissolution over the leaching period, Cs^+ released from the ion-exchange and adsorption by the geopolymer binder and possibly dissolution in the connected pore in the geopolymer binder and diffuse to the leachate. On the other hand, Si and Al remain the same intensity, even long-time leaching.

4.3.2.3 Ordinary Portland cement with Cs adsorbed titanate adsorbent

The leaching rate of Cs is shown in Table 4-3 and Figure 4-10, 33.41% Cs^+ leached to the system after 360 days leaching. The XRD patterns are similar in every leaching period sample. The crystalline peaks are related to peak of hardened ordinary Portland cement peaks with small broad features at around 9° 2θ from titanate adsorbent layer (Figure 4-11). From EPMA elemental maps of the specimen before leached (Figure 4-12, a),19 days (Figure 4-12, b), 90 days (Figure 4-12, c), and 360 days (Figure 4-12, d) leached, Ti and Na distributions indicate the adsorbent areas. High intensity of Na and Cs is evident in the adsorbent area before leaching specimens and continuously abate after leaching age. Converse with Ca, which is small intensity in the adsorbent area of 0-day leaching specimen and increasingly over a long period, supporting more favorable Ca^{2+} on titanate adsorbent than Cs^+ and Na^+ and consequence the elimination of Cs from the specimen.

4.3.2.4 Ordinary Portland cement-Cs without titanate adsorbent

The result showed a very voluminous leaching rate; almost 80% of Cs^+ leached out after 360 leaching days, as expressed in Table 4-4 and Figure 4-13. The XRD patterns (Figure 4-14) show mainly hardened OPC phase crystalline peaks with identical peaks among the different leaching periods. EPMA elemental maps, focusing on Cs (Figure 4-15), showed high element distribution in the matrix and reduced after lengthened leaching period indicating the weak retention for Cs^+ by ordinary Portland cement paste.

4.3.3 Comparison of retention efficiency of the waste forms with Cs

Figure 4-16 shows the efficiency of the retention of Cs^+ inside the geopolymer matrix compared with the geopolymer specimen without titanate adsorbent and specimens of ordinary Portland cement (OPC) with and without titanate adsorbent on a log scale against leach time in days. After 360 days of leaching, 11.38% of the introduced Cs^+ was released from the geopolymer specimen with the absence of titanate adsorbent, and the leach rate also rapidly increased in the early period of leaching. Indicating the initial surface of the sample is typically wash-off and comprises the fast dissolution of soluble elements from the surface (A van der sloot and Dijkstra, 2004), and possible diffusion-controlled release after the initial leaching period. Moreover, Cs^+ slightly reacts with aluminate phases and replace K^+ during the formation of the geopolymer (Skorina, 2014), (Kuenzel et al., 2015), (Komljenovi et al., 2020) and suggested the immobilization capacities depend on Si/Al ratio of the matrix which expresses higher capacity with low Si/Al ratio (the lowest value at Si/Al of 2) and decrease capacity when gradual increase Si/Al ratios higher than 3 (Aly et al., 2008), (Vandevenne et al., 2018). Besides, it is possibly incorporated into the alkaline aluminosilicate gel and become the Cs-aluminosilicate, pollucite, in the framework structure (Ito, 1976), (Fernández-Jiménez et al., 2005).

The leaching rate of OPC with titanate adsorbent (33.41% after 360 days) and without adsorbent (79.86% after 360 days) were utterly higher than the geopolymer matrix. With the adsorbent, Cs^+ showed less preferentially remain on titanate for Ca^+, which is concentrated in the cement matrix. Because of a lower valence and higher radii size of Cs^+ over Ca^{2+} (Lehto et al., 1999). The different leaching rates between the specimen with and without adsorbent may be attributed to the high surface area of adsorbent which is capable of reducing the volume of large pores and capillaries founded in cement pastes (El-Kamash et al., 2006). After the Cs^+ is exchanged from the adsorbent

into the cement matrix, the degree of retention of Cs^+ in the ordinary Portland cement matrices is deficient and easily diffusion towards the environment (Khalil and Merz, 1994), (Goni et al., 2006), (Ochs et al., 2006), (Rahman et al., 2007). Definitely, OPC has low efficiency in retaining Cs^+, following the experimental results, revealed the high amount of Cs^+ leached from the cement specimens.

4.4 Conclusions

This study presented the great selectivity for Cs^+ on titanate adsorbent with the stable in both physical and chemical properties during embedding in geopolymer binder and through the leaching processes. The encapsulation of adsorbent with a realistic Cs concentration in alkali-activated metakaolin with a potassium silicate activator shows satisfactory performance for retaining Cs. The experimental results have shown that 6.92% of Cs leached after 360 days of leaching regarding the high K content of the system can affect and exchange with Cs on the titanate adsorbent and geopolymer framework. However, Cs leaching rate of geopolymer matrix with titanate adsorbent expressed the optimum value compared with the other kinds of specimens. In general, the geopolymer with Cs-loaded titanate adsorbent is promising for optional waste immobilization purposes. Also, a deeper understanding of the immobilization mechanism of Cs in titanate adsorbent could encourage further research and large-scale applications.

Figure 4-1 Field Emission-Electron Probe Micro Analyzer (FE-EPMA)

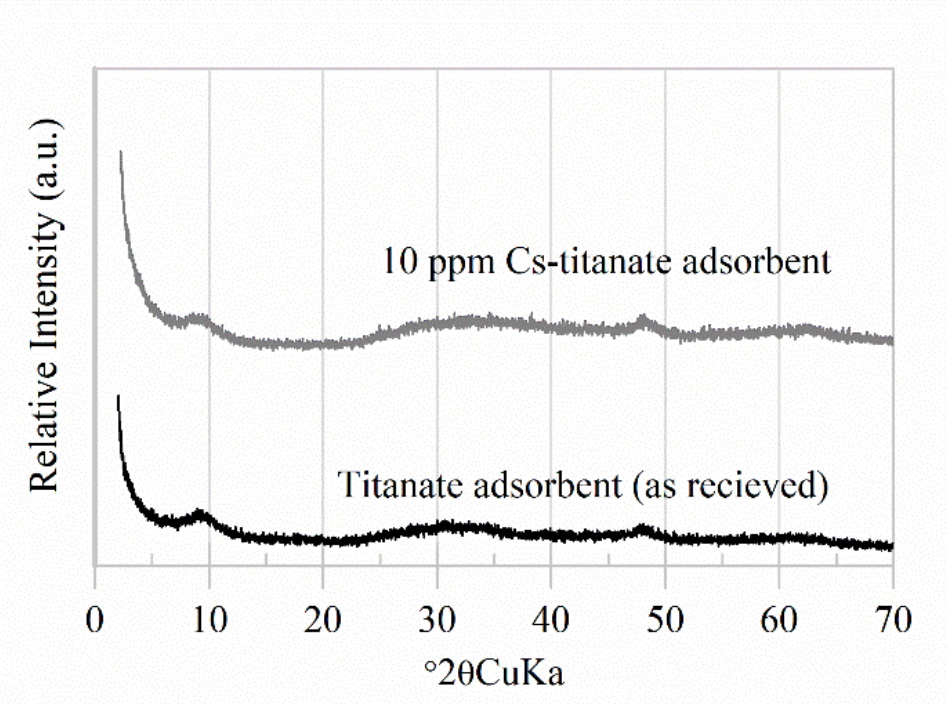

Figure 4-2 XRD patterns of titanate adsorbent before and after loading with Cs^+

Table 4-1 Cumulative leaching of Cs^+ from geopolymer with titanate adsorbent from each leach time

Leach time (days)	Cumulative leached rate (%)
0.083 (2 hours)	0.72
0.292 (7 hours)	1.34
1	2.22
2	2.70
3	2.96
4	3.17
5	3.36
19	4.75
47	5.30
90	5.62
150	6.02
210	6.29
270	6.56
330	6.79
360	6.92

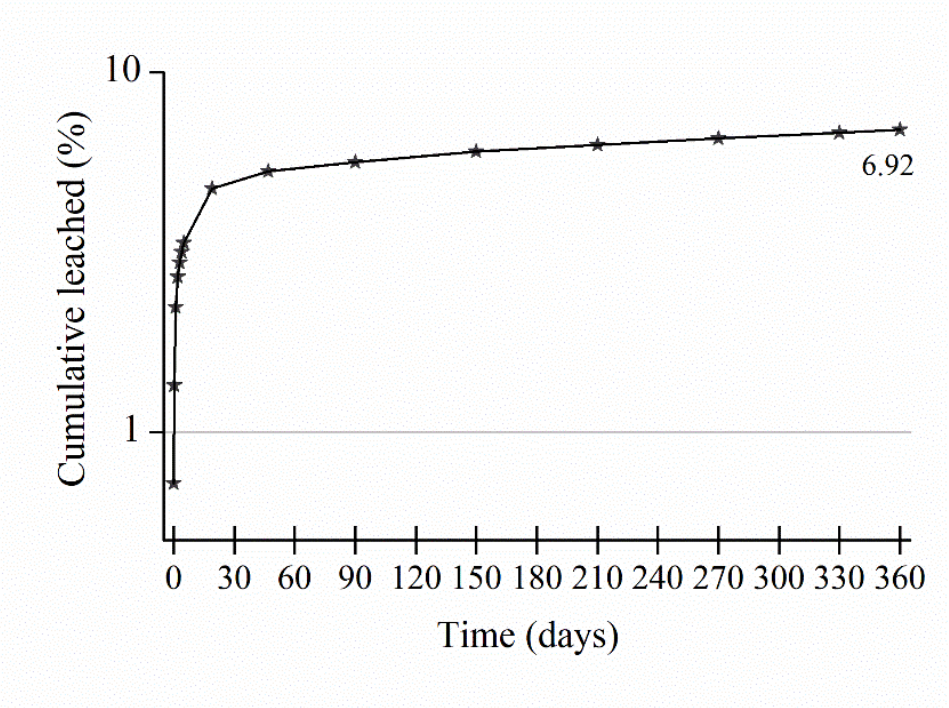

Figure 4-3 Cumulative leaching of Cs^+ from geopolymer mixed with titanate adsorbent, applying the ANSI/ANS 16.1 test method with full replacement of leachate at each sampling point shown

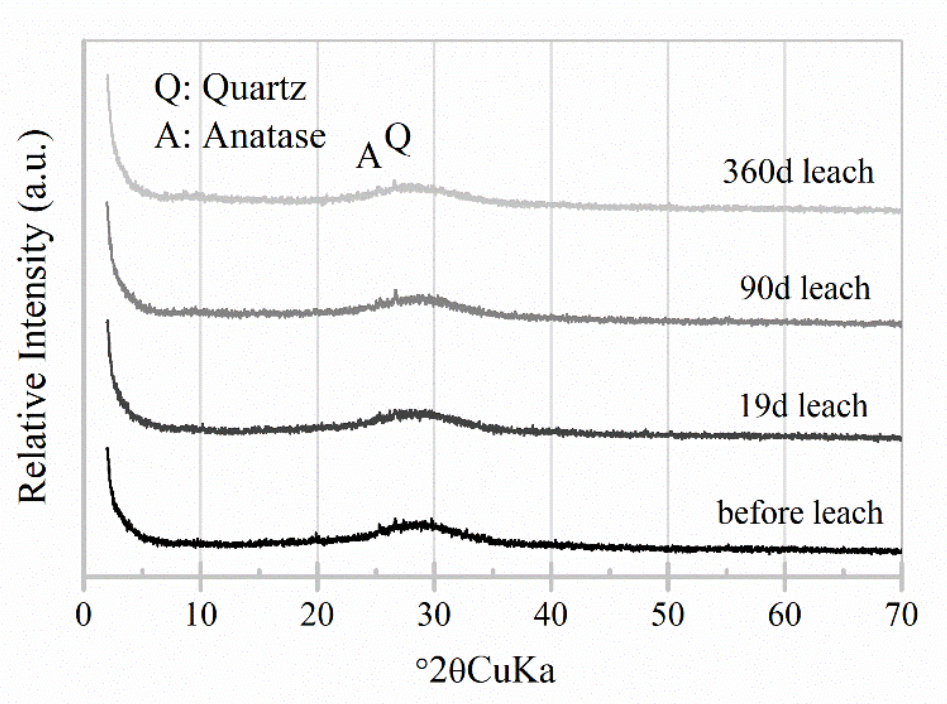

Figure 4-4 XRD patterns of K-geopolymer with spent titanate adsorbent loaded Cs before and after leaching for different durations as marked

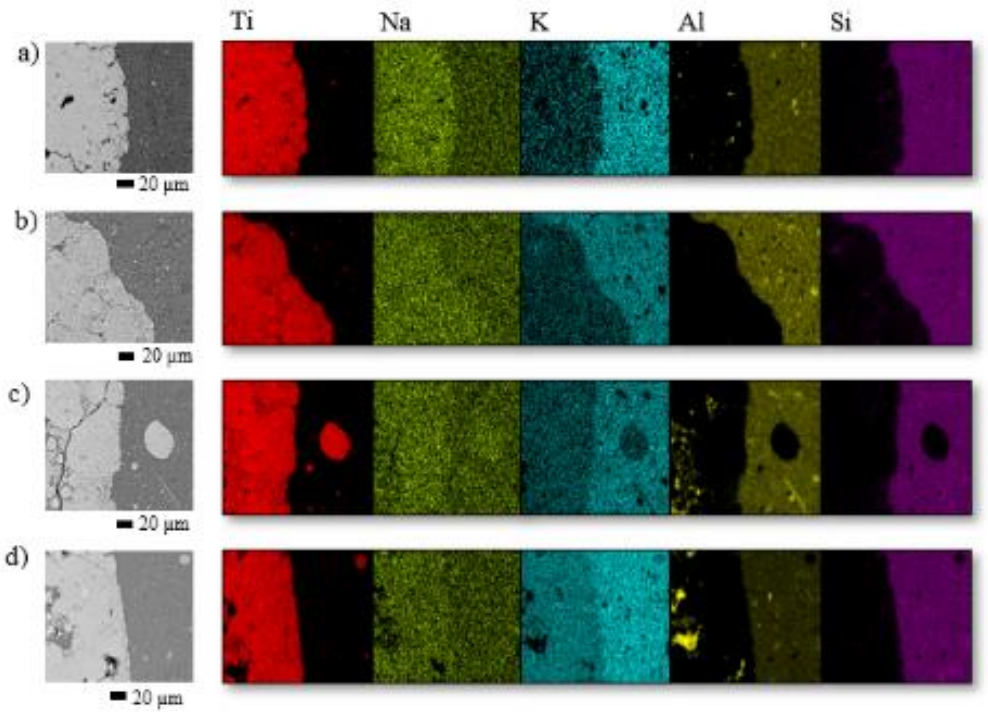

Figure 4-5 SEM images and elemental maps of geopolymer specimens with titanate adsorbent loaded Cs; a) before, and after b) 19days, c) 90days, and d) 360 days of leaching in deionized water

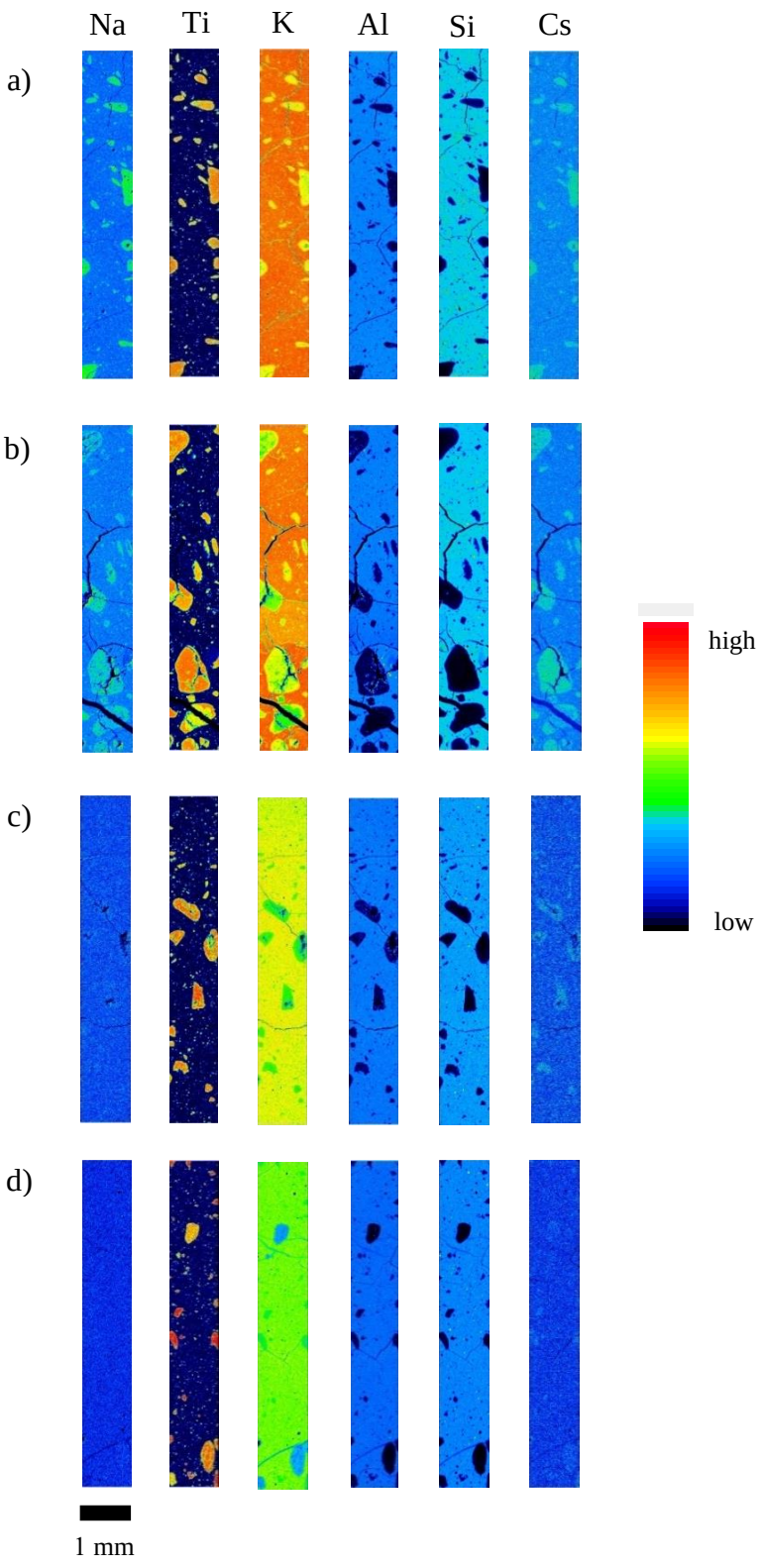

Figure 4-6 EPMA elemental maps of geopolymer specimens with titanate adsorbent loaded Cs; a) before, and after b) 19 days, c) 90 days, and d) 360 days of leaching in deionized water

Table 4-2 Cumulative leaching of Cs^+ from geopolymer without titanate adsorbent from each leach time

Leach time (days)	Cumulative leached rate (%)
0.083 (2 hours)	0.87
0.292 (7 hours)	1.54
1	2.42
2	3.03
3	3.45
4	3.70
5	3.95
19	5.49
47	6.91
90	8.14
150	9.26
210	9.94
270	10.51
330	11.04
360	11.38

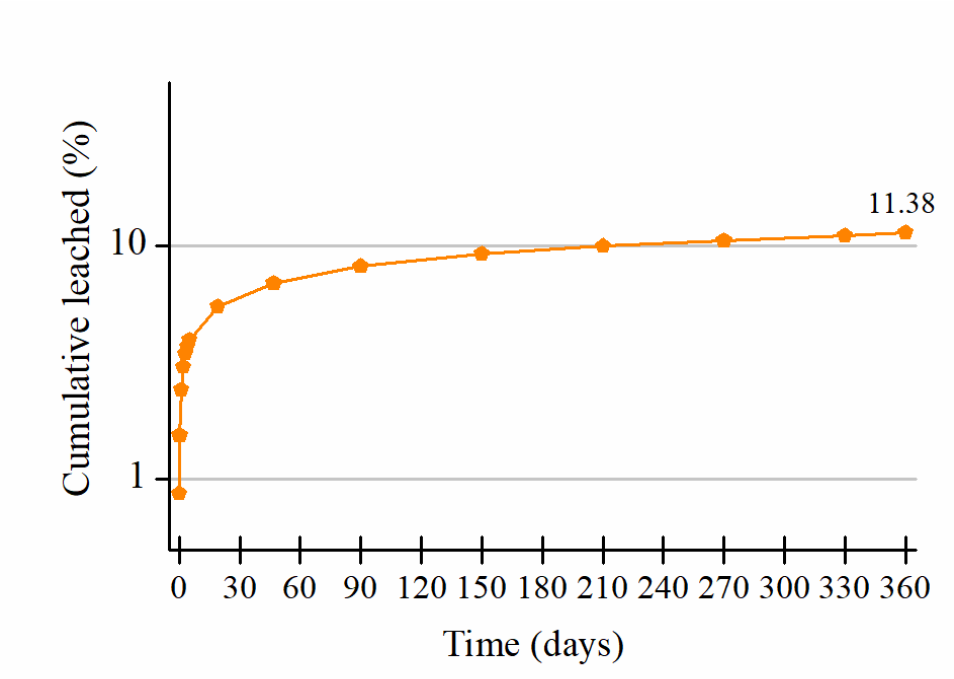

Figure 4-7 Cumulative leaching of Cs^+ from geopolymer without titanate adsorbent

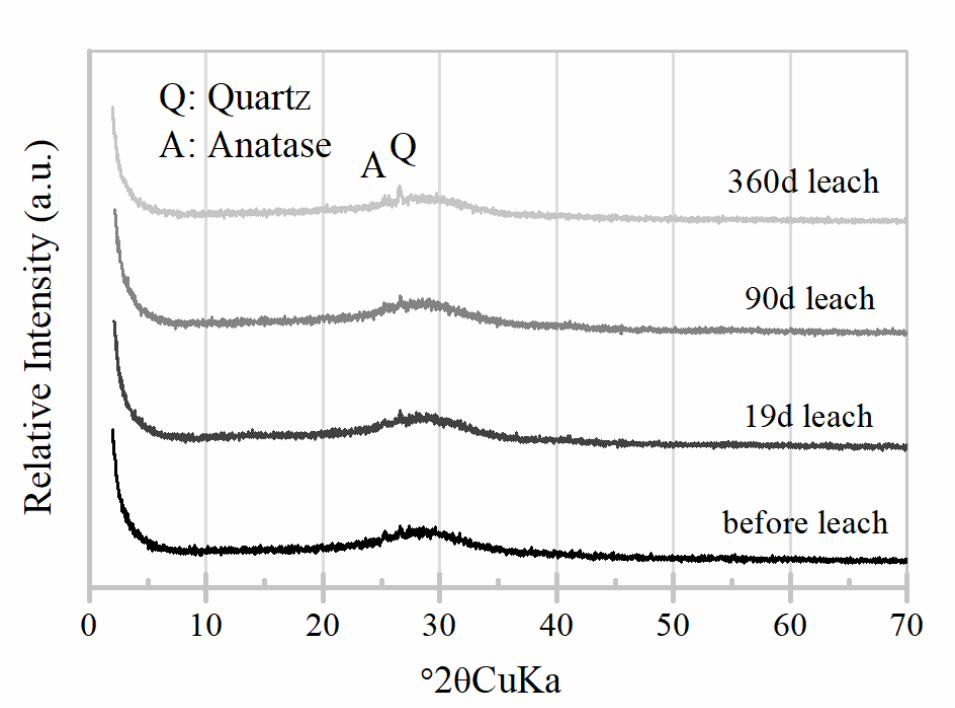

Figure 4-8 XRD patterns of K-geopolymer loaded Cs without spent titanate adsorbent before and after leaching for different durations as marked

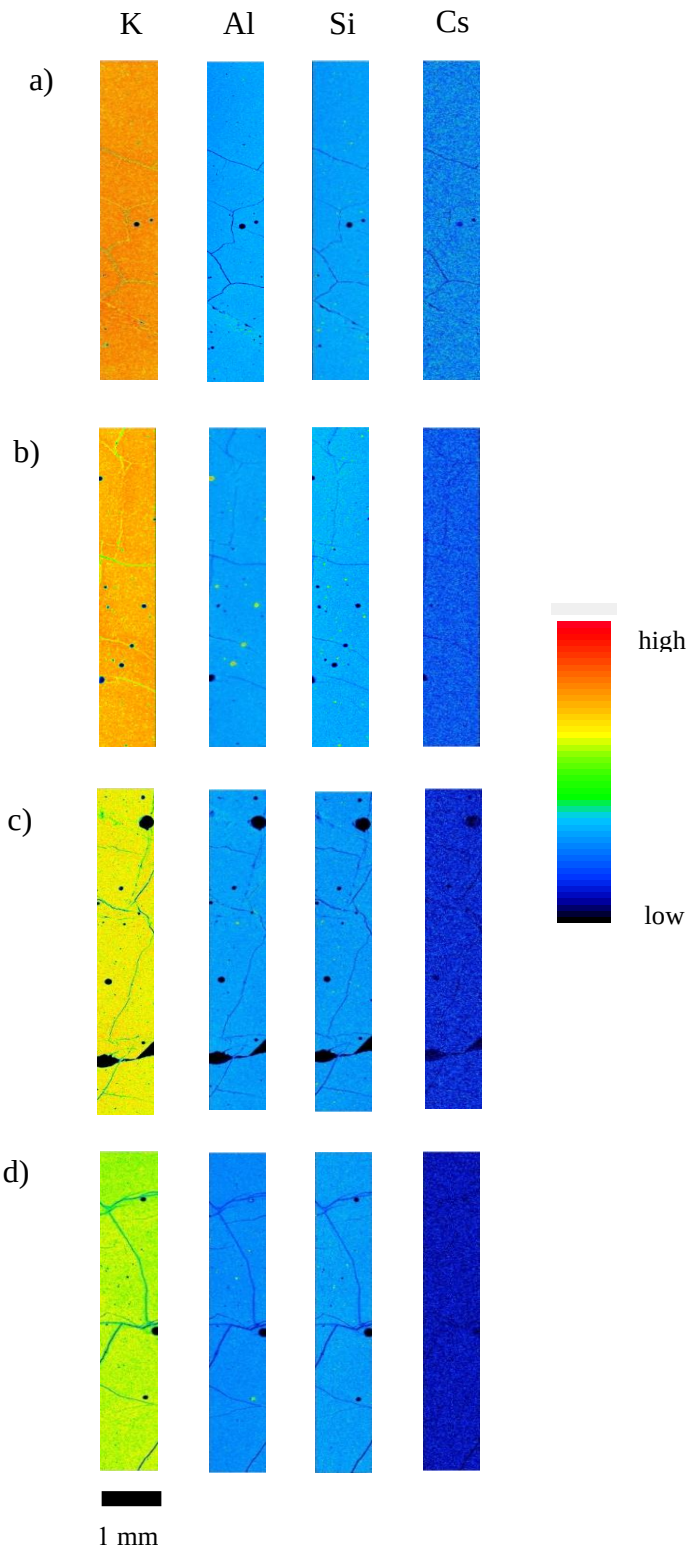

Figure 4-9 EPMA elemental maps of geopolymer specimens loaded Cs without titanate adsorbent; a) before, and after b) 19 days, c) 90 days, and d) 360 days of leaching in deionized

Table 4-3 Cumulative leaching of Cs^+ from ordinary Portland cement with titanate adsorbent from each leach time

Leach time (days)	Cumulative leached rate (%)
0.083 (2 hours)	1.54
0.292 (7 hours)	3.05
1	4.73
2	6.28
3	7.74
4	9.14
5	10.51
19	12.50
47	15.58
90	20.50
150	24.58
210	27.07
270	29.55
330	32.10
360	33.41

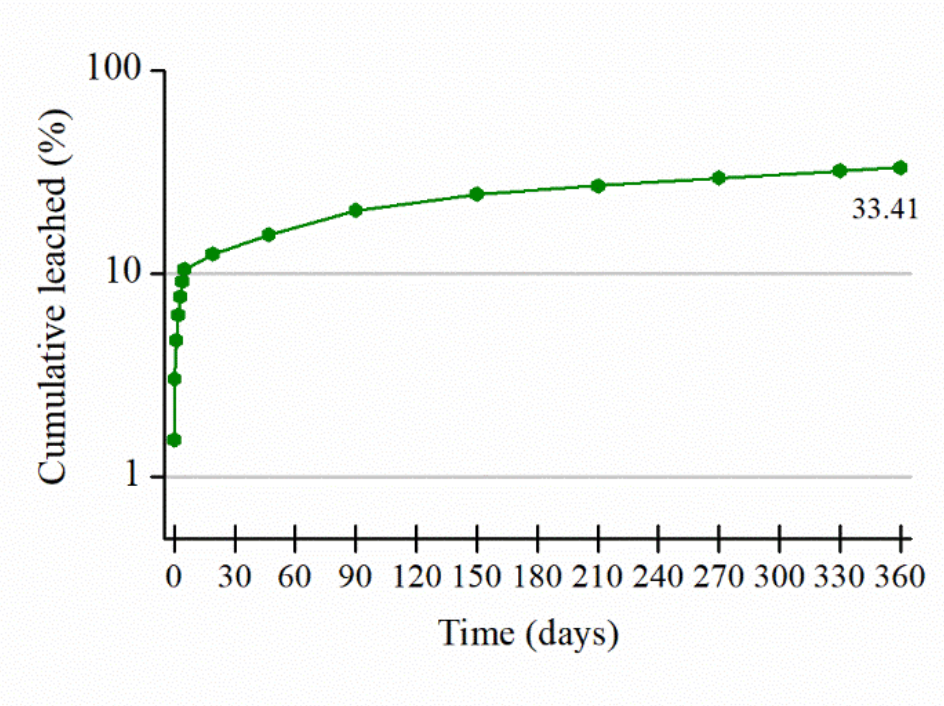

Figure 4-10 Cumulative leaching of Cs^+ from ordinary Portland cement with titanate adsorbent

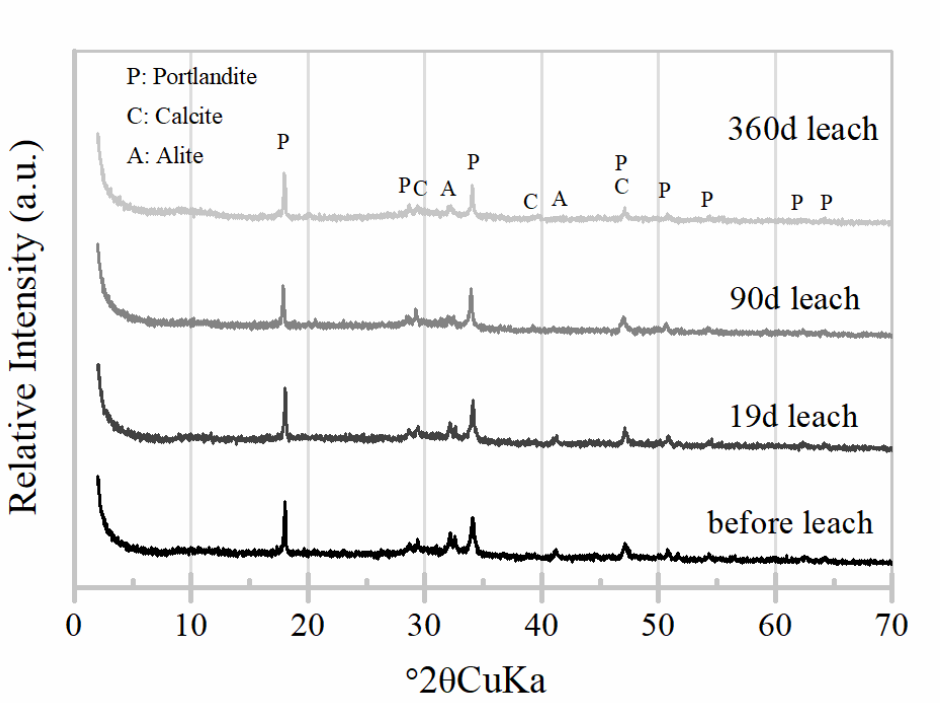

Figure 4-11 XRD patterns of ordinary Portland cement with spent titanate adsorbent loaded Cs before and after leaching for different durations as marked

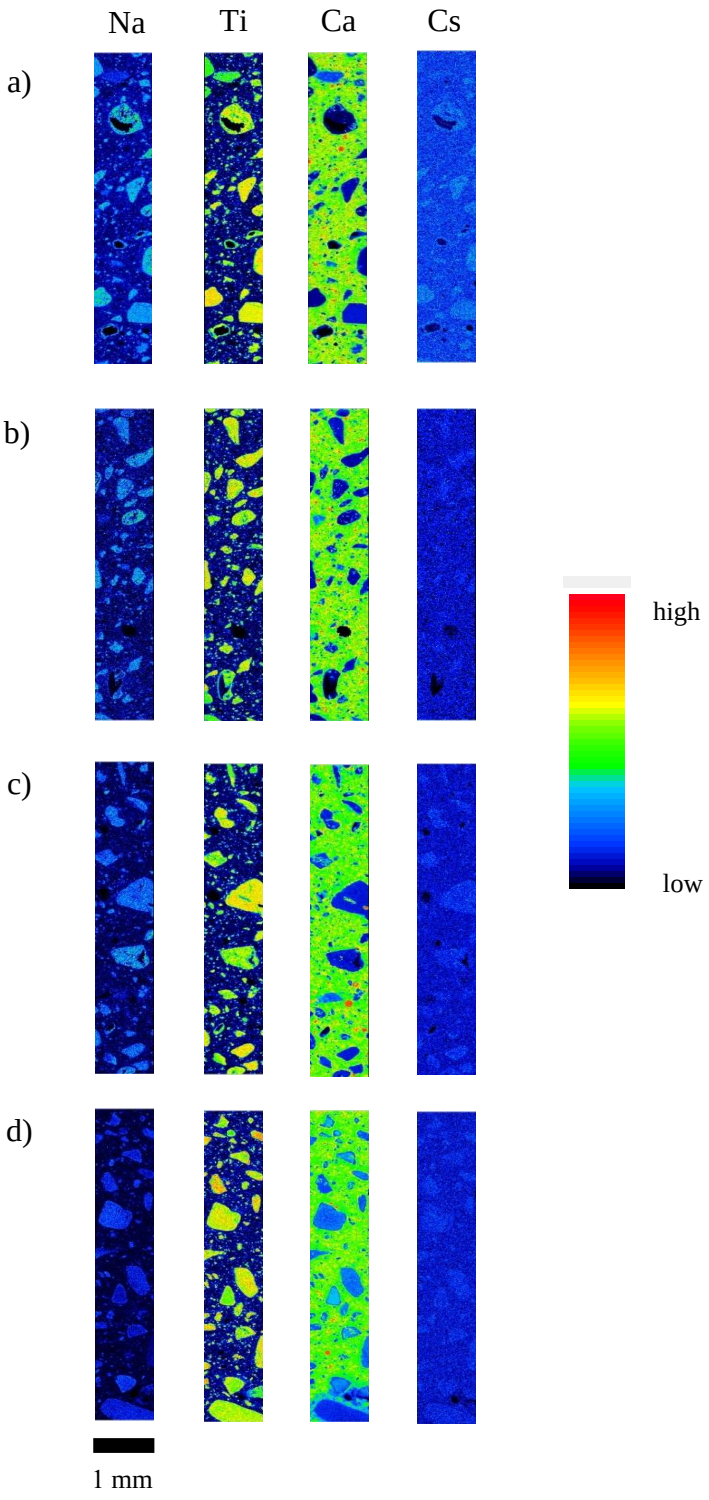

Figure 4-12 EPMA elemental maps of ordinary Portland cement specimens with titanate adsorbent loaded Cs; a) before, and after b) 19days, c) 90days, and d) 360 days of leaching in deionized water

Table 4-4 Cumulative leaching of Cs^+ from ordinary Portland cement without titanate adsorbent from each leach time

Leach time (days)	Cumulative leached rate (%)
0.083 (2 hours)	4.78
0.292 (7 hours)	6.67
1	9.79
2	12.65
3	14.90
4	16.74
5	18.30
19	29.55
47	39.59
90	49.89
150	56.37
210	63.61
270	69.68
330	77.24
360	79.86

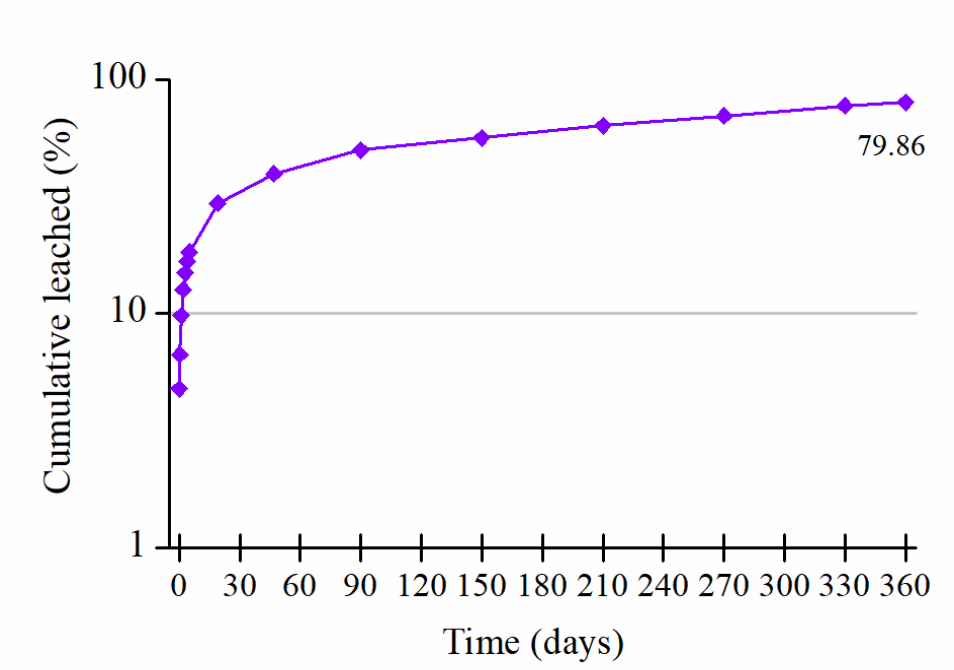

Figure 4-13 Cumulative leaching of Cs^+ from ordinary Portland cement without titanate adsorbent

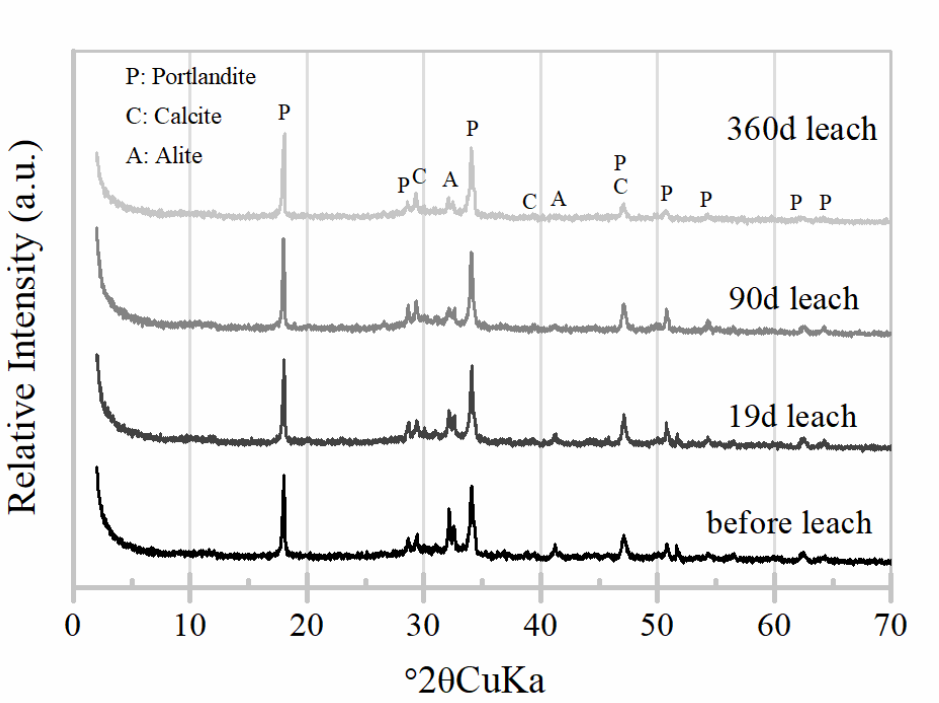

Figure 4-14 XRD patterns of ordinary Portland cement loaded Cs without spent titanate adsorbent before and after leaching for different durations as marked

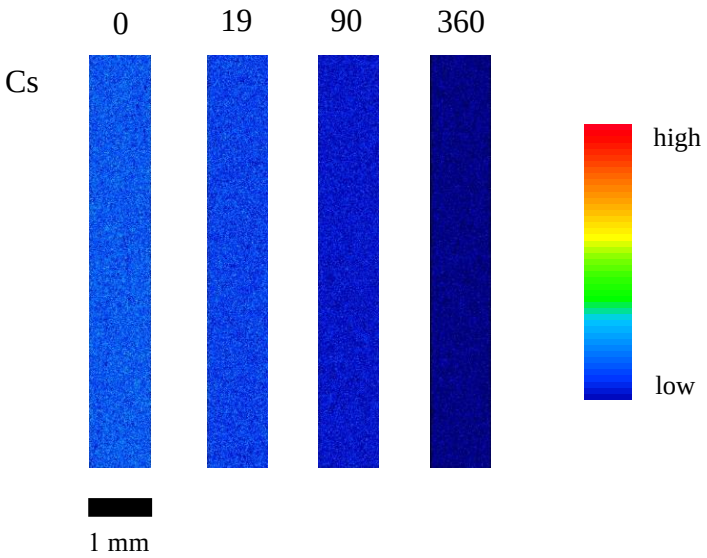

Figure 4-15 EPMA elemental maps of ordinary Portland cement specimens loaded Cs without titanate adsorbent before leaching in deionized water

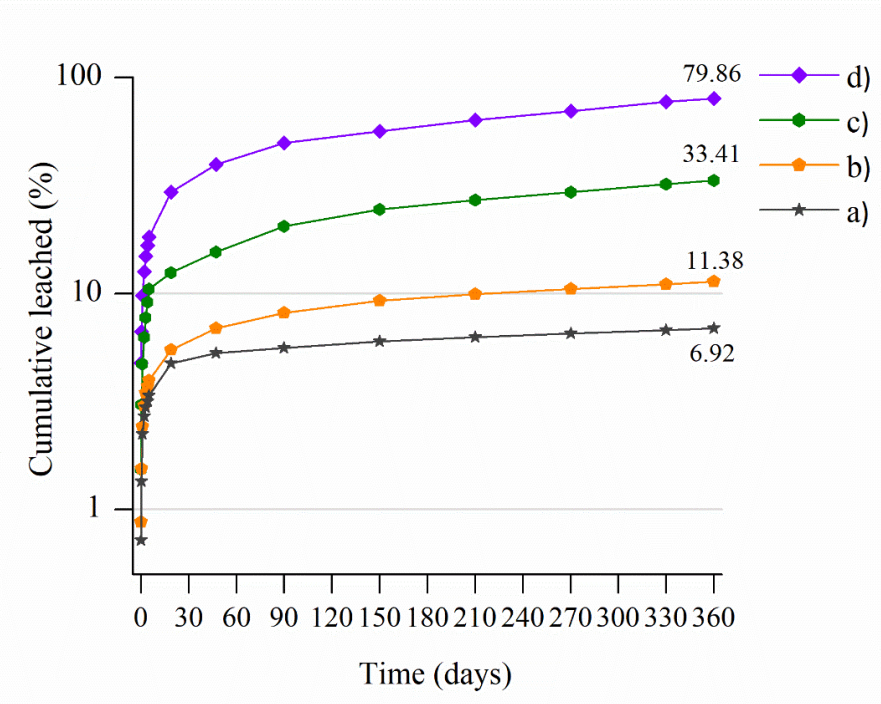

Figure 4-16 Cumulative leached percentage of Cs^+ from: a) geopolymer without adsorbent, b) geopolymer with adsorbent, c) cement with adsorbent, d) cement without adsorbent

Chapter 5: Safety assessment of geopolymer waste with titanate adsorbent loaded Sr/Cs

5.1 Introduction

In the previous chapter, the leaching rate of Sr and Cs from the geopolymer waste form with titanate adsorbent are known and showed a relatively low percentage of Sr leached out after 360 days leaching. However, it is a necessary to consider the suitable disposal system for the long-term storage of these wastes. Hence, a long-term environmental assessment of geological repository for a low-level radioactive waste arising from a reprocessing of contaminated water at Advanced Liquid Processing System (ALPS) in FDNPS is one of the critical issues for consideration.

To evaluate whether these disposal systems are actually applicable, a safety evaluation on a shallow underground pit and trench disposal system is conducted using GoldSim software, a platform for simulating complex environmental systems over time and predicting the future behavior of radionuclides. The evaluation is based on the standards of the Atomic Energy Society of Japan (AESJ) information for analyzing the exposure dose. Sr-90 (half-life 29.1 years) and Cs-137 (half-life 30 years) are identified as key distributors to measure the radiological dose using the 90 days leaching rate of Sr/Cs from geopolymer with titanate adsorbent specimens. With considered the groundwater migration scenario and land use scenario assumes as the direct and indirect major exposure routes which affect the environment and human life for the pit and trench disposal system. Varying the thickness of cover soil for pit type disposal and varying the management period towards the safety requirements to assess under the limitation of annual radiation dose and apply to the real situation.

5.2 Perspective of model system and parameters

5.2.1 Perspective of model system

Low-level radioactive waste (LLW) refers to a category of radioactive wastes that contain essentially short-lived (half-life not in excess of 30 years) with being limited to very small concentrations of radionuclides. The concentrations are diminutive enough that managing these wastes may not require all the radiation protection measures. In Japan, low-level radioactive waste is classified into four categories as follow (Nuclear Energy Agency, 1999) and show in Figure 5-1:

- Low-level radioactive waste for near-surface disposal without engineered barrier; Trench disposal (L3 waste)
- Low-level radioactive waste for near-surface disposal with engineered barrier; Pit disposal (L2 waste)
- Low-level radioactive waste for subsurface disposal with engineered barrier; Subsurface disposal (L1 waste)
- Low-level radioactive waste for geological disposal (TRU waste)

Low-level radioactive waste for near-surface disposal without engineered barrier; Trench disposal (L3 waste) and low-level radioactive waste for near-surface disposal with engineered barrier; Pit disposal (L2 waste) are considered for use as the disposal system in this study to assess the possibility for safe storage of geopolymer with titanate adsorbent specimens.

Trench disposal which is near-surface disposal facilities at ground level. These facilities are on or below the surface where the protective covering is a few meters thick. Waste containers are constructed basements and backfilled when full of the basements. Then, it will be covered and capped with an impermeable membrane and topsoil. These facilities may incorporate some form of drainage and possibly a gas venting system. The size of the trench considered in this study is 40 x 50 x 5 m. Alternatively, pit disposal, which is near-surface disposal facilities in caverns below ground level. The excavations are conducted from the surface, the facility is at a depth of several tens of meters below surface and accessed through a drift. 500 x 500 x 5 meters pit size is used in this study, covering a few meters of soil thickness.

The radiation exposure path considered in this assessment is concerned as a groundwater migration and land use scenarios. Groundwater migration scenario which assumes that the nuclides leaked from the disposal facility and transferred to the environment via groundwater. Eventually, the migration path of radionuclides remained in the rocks and groundwater around the buried facilities near the surface and possibly exposed to the living things. Different from land use scenarios, which assumes the direct radionuclides exposures by human and animal activities. The maximum exposure dose in each scenario was evaluated, and the exposure route with the maximum exposure dose is shown in Table 5-1.

5.2.2 Input parameters

Input parameters required to assess the environmental impact based on the standards of the Atomic Energy Society of Japan (AESJ) are shown in Table 5-2 with possibly have uncertainties on their estimated values.

5.3 Results and discussion of simulated data using GOLDSIM software

5.3.1 Simulated data of geopolymer with titanate adsorbent loaded Sr

Figure 5-2 Annual radiation dose (μSv/year) against time (years) of a geopolymer-titanate-Sr specimen in the groundwater migration scenario for pit disposalshows the environmental impact of Sr radionuclides from annual radiation dose (μSv/year) against the time period (years) in the groundwater migration scenario for pit disposal, varying the differences in soil thickness cover and the management period using maximum inventory for simulation. The annual exposure dose is changed under varying conditions, the lower thickness of soil cover and management period give a higher annual exposure dose. Suggested the soil cover restricted the radionuclides. The highest annual exposure dose is 4.84 E-1 μSv/year on 0.5 meters thickness of soil cover and 0-year management period which is below the limitation level of radiation exposure dose (10 μSv/year ((Nuclear Regulatory Authority of Japan, 2013), (Nakabayashi and Sugiyama, 2017)). These indicated the safe storage way for geopolymer with titanate adsorbent loaded Sr is suitable in all variations pit type disposal.

Trench disposal in groundwater migration scenario varying the management period using maximum inventory for simulation, the annual exposure dose significantly exceeded the limitation dose of 10 μSv/year indicated by red dash line (Figure 5-3) since soil covering used as an artificial barrier layer is not used in this disposal system. The highest annual exposure dose is 1.66 E+7 μSv/year and considered the trench disposal is inappropriate as a disposal system for solidified geopolymer of titanate adsorbent.

In the land use scenario, the annual exposure dose for pit disposal varies in the thickness of soil cover, and the management period using maximum inventory for simulation is shown in Figure 5-4. The highest annual exposure dose is 8.13 E-2 μSv/year on 0.5 meters thickness of soil cover and 0-year management period (similar to groundwater migration scenario). The results obtained below the target dose indicated by red dash line in all conditions. It considered being sufficiently

attenuated of radionuclide before the facility reaches near the surface. Moreover, all conditions are lower than the groundwater migration scenario.

As for trench disposal (Figure 5-5), the annual exposure dose shows a high overdose from the target doses the same as in the water migration scenario. The radionuclide activities are not restricted with the highest exposure dose of 1.7 E+9 μSv/year.

5.3.2 Simulated data of geopolymer with titanate adsorbent loaded Cs

On the groundwater migration scenario, the simulation showed the environmental impact of Cs from annual radiation dose (μSv/year) against the time (years) in the groundwater migration scenario for pit disposal (Figure 5-6). The radiation dose of 0.5 meters thickness of soil cover on 0- and 50-years management period are over the limitation level of radiation exposure dose with lower in the others variation. In the case of land use scenario (Figure 5-8), only 0.5 meters thickness of soil cover on the 0-year management period is slightly over the limit. Moreover, trench disposal in groundwater migration scenario (Figure 5-7) and land use scenario (Figure 5-9), the annual exposure dose significantly exceeded the limitation dose. Those cases mentioned above are not appropriate for utilization as a disposal system for a solidified geopolymer with titanate loaded Cs.

5.4 Conclusions

The safety evaluation conducted this time revealed that it is effective to adopt pit disposal as a disposal system for the solidified geopolymer of titanate generated in the treatment processes of contaminated water, and the target nuclide is Sr-90. It was confirmed that the maximum exposure dose was below the limitation dose in the safety evaluation. However, over the 0.5 meters thickness of soil cover are applicable in Cs radionuclides.

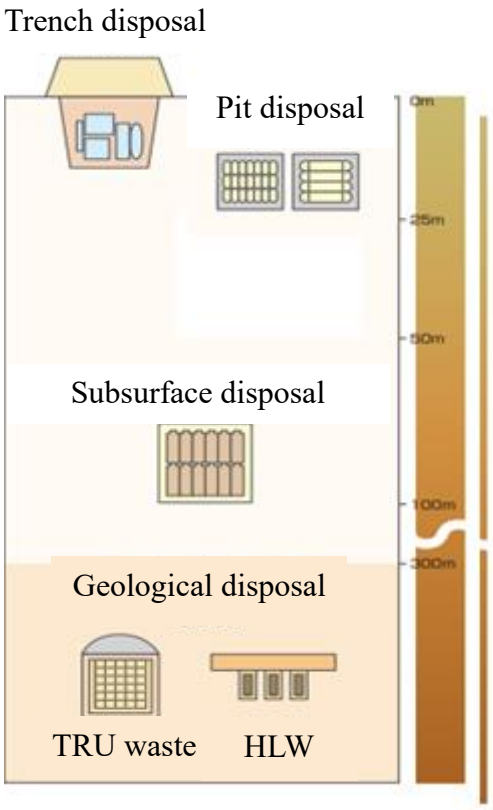

Figure 5-1 The classification of disposal facilities of low-level radioactive waste

Table 5-1 The maximum exposure route in each scenario with different disposal types

			Maximum exposure route
Titanate_Sr	Groundwater migration scenario	Trench disposal	Internal exposure from ingestion of animal grew using feed irrigated soil
		Pit disposal	Internal exposure from consumption of crops grow in irrigated soil
	Land use scenario	Trench disposal	Internal exposure due to crop consumption by farming on topsoil
		Pit disposal	Internal exposure due to crop consumption by farming on topsoil
Titanate_Cs	Groundwater migration scenario	Trench disposal	Internal exposure from ingestion of animal grew using feed irrigated soil
		Pit disposal	Internal exposure due to intake of marine products from rivers
	Land use scenario	Trench disposal	External exposure of construction workers by an excavation of soil covering
		Pit disposal	External exposure of construction workers by an excavation of soil covering

Table 5-2 Input parameters for safety assessment evaluation

Parameters		Values
Leaching rate (90 days)	Geopolymer-titanate-Sr	0.58 %
	Geopolymer-titanate-Cs	5.62 %
Estimated inventory	1.00 E+18 [Bq]	
Management period	Trench disposal	0, 50 years
	Pit disposal	0, 50, 300 years
Thickness of soil cover	Pit disposal	0.5, 1, 2 meters

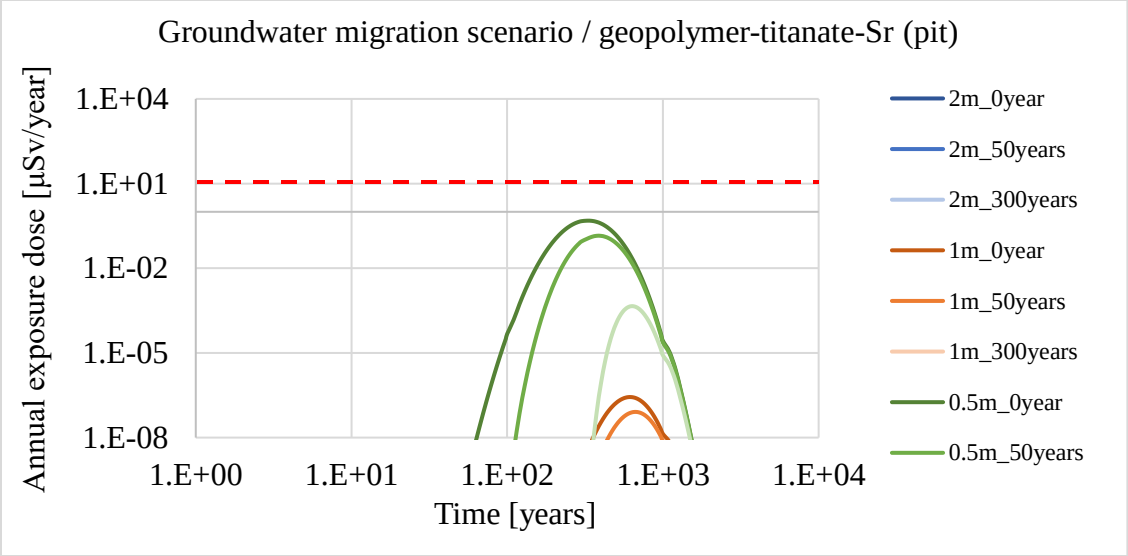

Figure 5-2 Annual radiation dose (μSv/year) against time (years) of a geopolymer-titanate-Sr specimen in the groundwater migration scenario for pit disposal

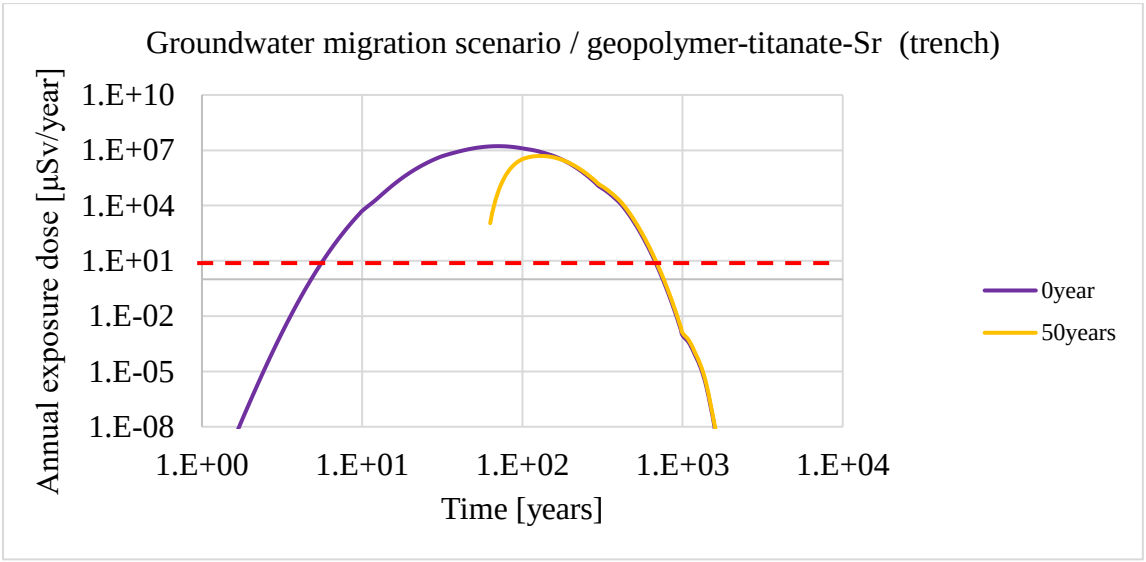

Figure 5-3 Annual radiation dose (μSv/year) against time (years) of a geopolymer-titanate-Sr specimen in the groundwater migration scenario for trench disposal

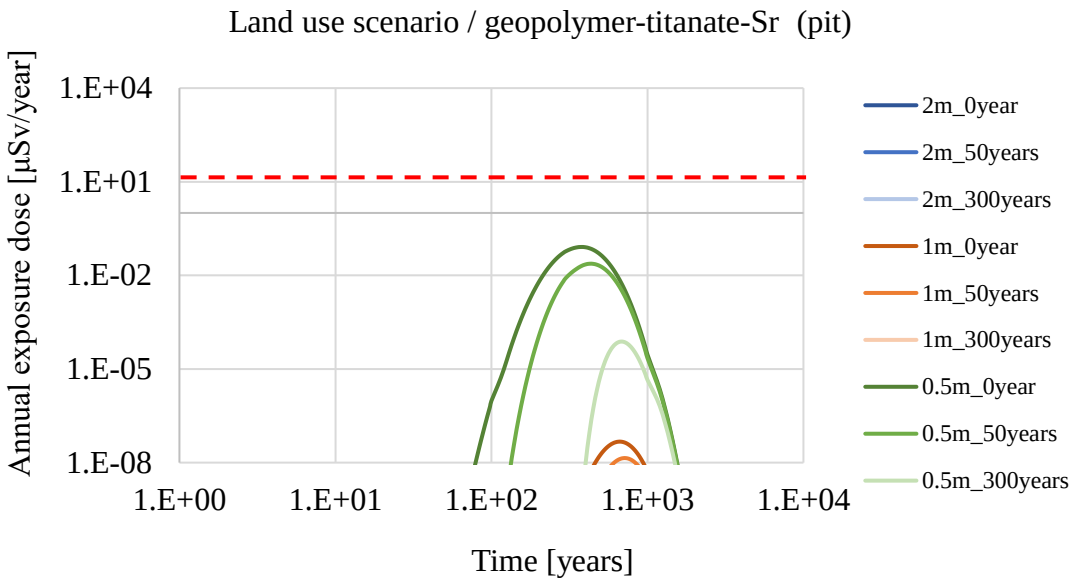

Figure 5-4 Annual radiation dose (μSv/year) against time (years) of a geopolymer-titanate-Sr specimen in the land use scenario for pit disposal

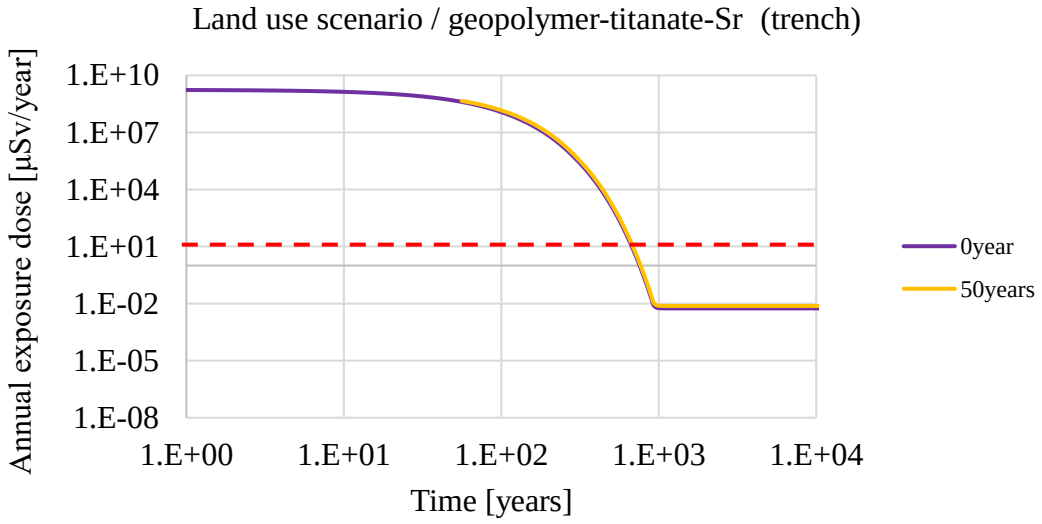

Figure 5-5 Annual radiation dose (μSv/year) against time (years) of a geopolymer-titanate-Sr specimen in the land use scenario for trench disposal

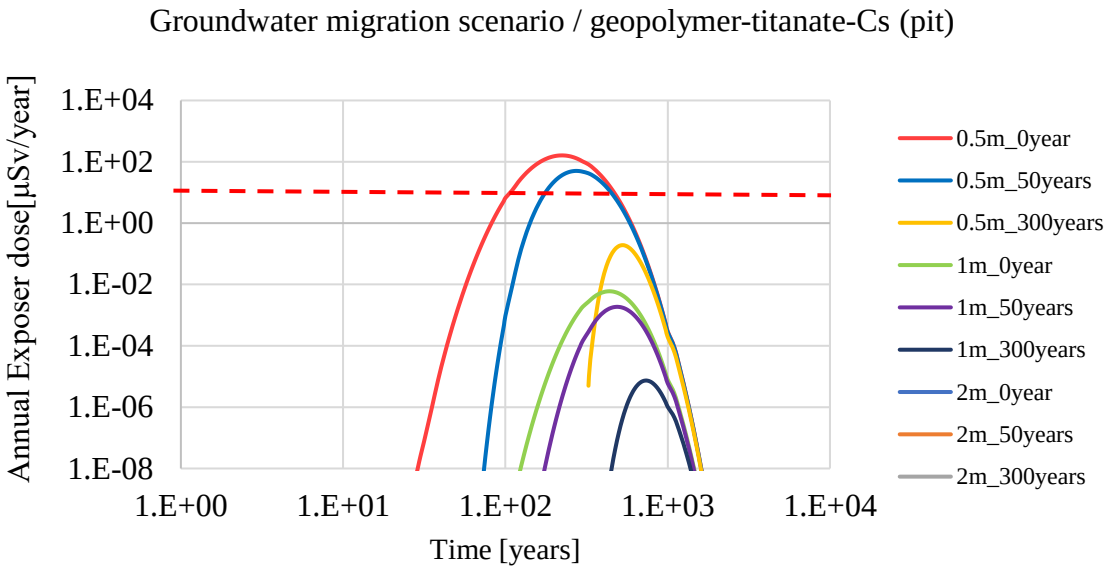

Figure 5-6 Annual radiation dose (μSv/year) against time (years) of a geopolymer-titanate-Cs specimen in the groundwater migration scenario for trench disposal

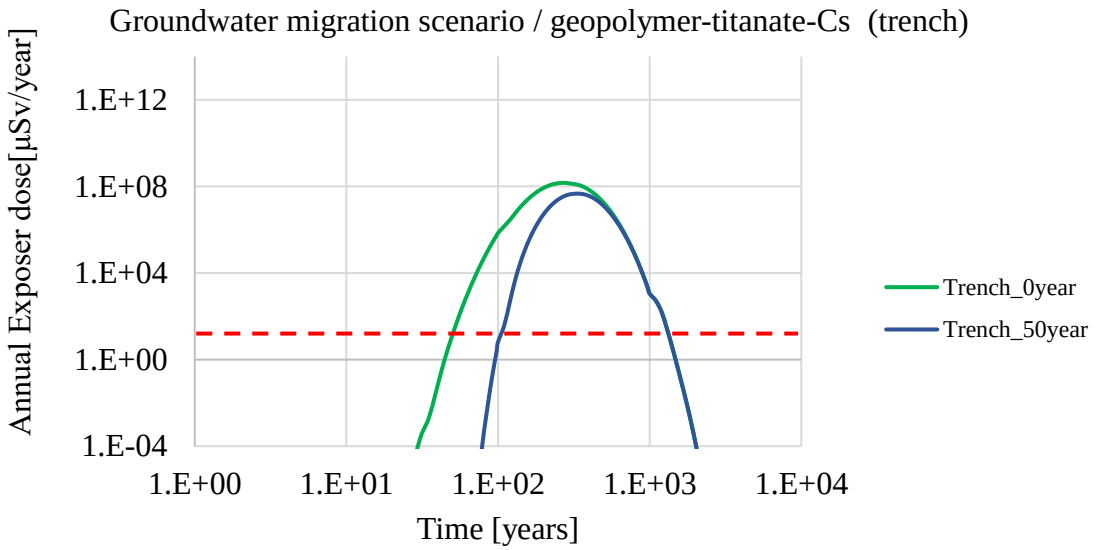

Figure 5-7 Annual radiation dose (μSv/year) against time (years) of a geopolymer-titanate-Cs specimen in the groundwater migration scenario for trench disposal

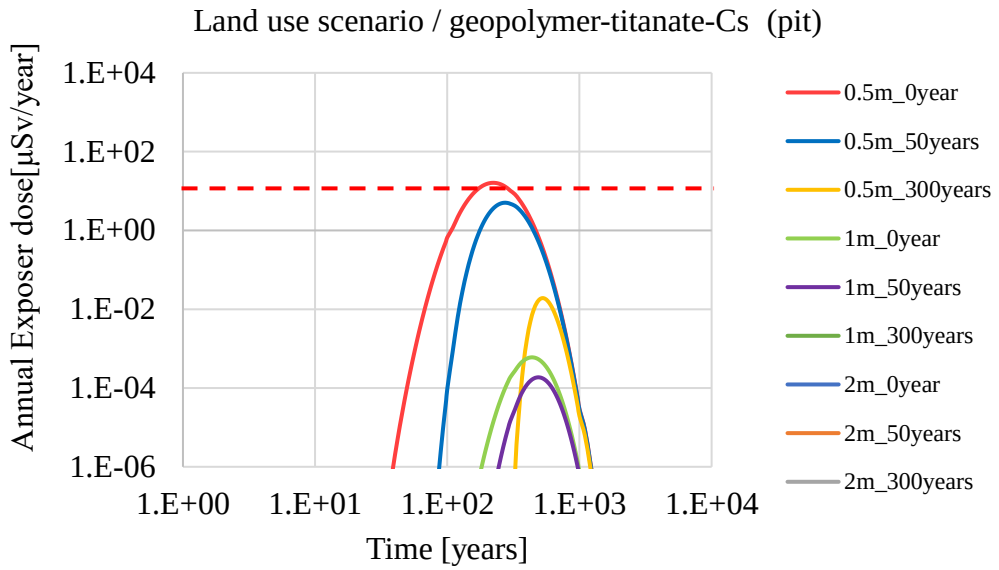

Figure 5-8 Annual radiation dose (μSv/year) against time (years) of a geopolymer-titanate-Cs specimen in the land use scenario for pit disposal

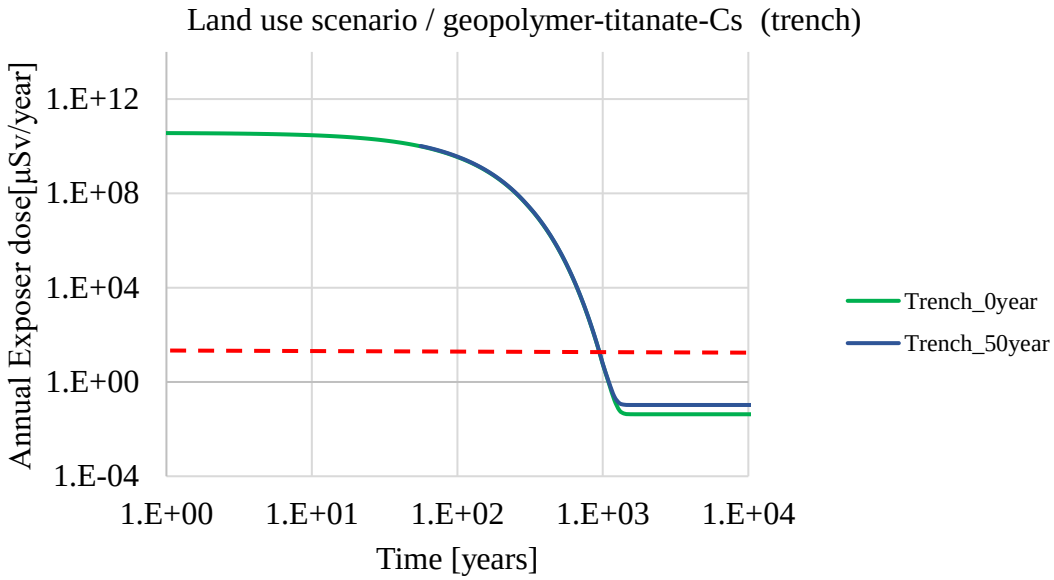

Figure 5-9 Annual radiation dose (μSv/year) against time (years) of a geopolymer-titanate-Cs specimen in the land use scenario for trench disposal

Chapter 6: General conclusions and recommendations

6.1 General conclusions

Titanate adsorbent has selectivity preferentially for alkali cations in order of Sr > Cs, presumably by the differentiating factors of each cation, such as valence, hardness, and radius. After adsorption with a relatively low Sr and Cs concentration, a stable constituent without different crystalline phases and precipitation appears. Then, embedded the loaded Sr and Cs into K-based metakaolin geopolymer, the leaching experiment and observation of Sr and Cs distribution on a metakaolin-based geopolymer were examined. Geopolymer with titanate adsorbent shows very effective Sr^{2+} immobilization, which is very promising for the use of alkali-activated material for the waste immobilization purposes with less potential for exchange by the other cations in the system. Sr strongly retains in titanate adsorbent part, no evidence of precipitation, and no phase change. As for Cs, inside the geopolymer with titanate adsorbent, the interference with K^+ slightly affects and exchanges with Cs^+ on the titanate adsorbent cause the gradual release of Cs^+ to the geopolymer matrix. To conclude with, the selectivity among several cations on the titanate adsorbent is conveyed in the following order: $H^+ >> Sr^{2+} \approx Ca^{2+} >> Cs^+ \approx K^+ > Na^+$.

The (low concentration) radionuclides reaction with a metakaolin-based geopolymer examined the feasible release of radionuclides from the titanate particle, Sr^{2+}, and Cs^+ ions are simply accommodated within a geopolymer framework and do not crucially transform the structure. Moreover, in order to compare with cementitious materials, major Ca^{2+} in the pore solution of the ordinary Portland cement matrix leads to arise a significant impact. On the titanate adsorbent inside the OPC matrix, less significantly different from the behavior between Ca^{2+} and Sr^{2+}, while Ca^{2+} has a massive impact with Cs^+. Subsequent, the Sr^{2+} and Cs^+ are leached or exchanged into the cement binder, Ca^{2+} shows superiority preference than Sr^{2+} and Cs^+ for replacing and binding to generate cement phases.

As for the safety assessment aspects, these geopolymers with the spent titanate adsorbents are suitable and safe for use as the waste form for long-term storage and disposal in shallow underground pit disposal. Underlying that K-geopolymers are excellent candidates as a waste matrix destined for long term storage and disposal of spent titanate adsorbent.

6.2 Recommendations for future work

Exploration of the optimum solidified waste form for encapsulation radionuclides over the consideration of long-term and safety storage is a great challenge and should brainstorm. Based on the experiences gained from this study, the weaknesses and limitations from this study should be developed according to the following recommendations and considerations:

a. The conduct of in-depth details on the adsorption of titanate adsorbent to evident the possibly different microstructure before and after radionuclides adsorption, which cannot show from XRD results.

b. Consider the physical properties of the matrix, such as compressive strength, surface area, pore size distribution by varying the mixing ratio, curing time, and so on. These can be tailored for scrutinizing the optimum properties of the solidified waste form.

c. Further work on the different types of leachant such as groundwater, rainwater, and seawater needed to be performed to fully assess the leaching behavior from the geopolymer matrix in the disposal environment.

d. Details on the structure of specimens from the analysis, such as solid-state nuclear magnetic resonance (NMR), Fourier-transform infrared spectroscopy (FT-IR), to observe the structure orienting and bond associating.

References

A van der sloot, H., Dijkstra, J.J., 2004. Development of horizontally standardized leaching tests for construction materials: a material or release based approach? Identical leaching mechanisms for diferrent materials. https://doi.org/10.13140/RG.2.2.11986.76486

Abdullah, M.M.A.B., Ming, L.Y., Yong, H.C., Tahir, M.F.M., 2018. Clay-based materials in geopolymer technology. Cement Based Materials. https://doi.org/10.5772/intechopen.74438

Ali, I.M., 2004. Synthesis and sorption behavior of semicrystalline sodium titanate as a new cation exchanger. Journal of Radioanalytical and Nuclear Chemistry 260, 149–157. https://doi.org/10.1023/B:JRNC.0000027074.36548.29

Aly, Z., Vance, E.R., Perera, D.S., Hanna, J. V, Griffith, C.S., Davis, J., Durce, D., 2008. Aqueous leachability of metakaolin-based geopolymers with molar ratios of Si / Al = 1.5–4 378, 172–179. https://doi.org/10.1016/j.jnucmat.2008.06.015

American Nuclear Society, 2004. Measurement of the leachability of solidified low-level radioactive wastes by a short-term test procedure ANSI/ANS-16.1-2003.

Atkins, M., Glasser, F.P., 1992. Application of portland cement-based materials to radioactive waste immobilization. Waste Management 12, 105–131. https://doi.org/10.1016/0956-053X(92)90044-J

Barbosa, V.F.F., Mackenzie, K.J.D., Thaumaturgo, C., 2000. Synthesis and characterisation of materials based on inorganic polymers of alumina and silica : sodium polysialate polymers. International Journal of Inorganic Materials 2, 309–317.

Bart, F., Cau-di-Coumes, C., Frizon, F., Lorente, S., 2013. Cement-based materials for nuclear waste storage. Springer New York. https://doi.org/10.1007/978-1-4614-3445-0

Bernal, S.A., Provis, J.L., 2014. Durability of alkali-activated materials: Progress and perspectives. Journal of the American Ceramic Society 1008, 997–1008. https://doi.org/10.1111/jace.12831

Blackford, M.G., Hanna, J. V, Pike, K.J., Vance, E.R., Perera, D.S., 2007. Transmission electron microscopy and nuclear magnetic resonance studies of geopolymers for radioactive waste immobilization 1199, 1193–1199. https://doi.org/10.1111/j.1551-2916.2007.01532.x

Davidovits, J., 1994. Properties of geopolymer cements, in: Proceedings First International Conference on Alkaline Cements and Concretes. pp. 131–149.

Duxson, P., Fernández-Jiménez, A., Provis, J.L., Lukey, G.C., Palomo, A., Van Deventer, J.S.J., 2007. Geopolymer technology: The current state of the art. Journal of Materials Science 42, 2917–2933. https://doi.org/10.1007/s10853-006-0637-z

Duxson, P., Provis, J.L., Lukey, G.C., Mallicoat, S.W., Kriven, W.M., Van Deventer, J.S.J., 2005. Understanding the relationship between geopolymer composition, microstructure and mechanical properties. Colloids and Surfaces A: Physicochemical and Engineering Aspects 269, 47–58. https://doi.org/10.1016/j.colsurfa.2005.06.060

El-diadamony, H., Amer, A.A., Sokkary, T.M., El-Hoseny, S., 2016. Hydration and characteristics of metakaolin pozzolanic cement pastes. HBRC Journal 14, 150–158. https://doi.org/10.1016/j.hbrcj.2015.05.005

El-Kamash, A.M., El-Naggar, M.R., El-Dessouky, M.I., 2006. Immobilization of cesium and strontium radionuclides in zeolite-cement blends. Journal of Hazardous Materials 136, 310–316. https://doi.org/10.1016/j.jhazmat.2005.12.020

Fernández-Jiménez, A., Macphee, D.E., Lachowski, E.E., Palomo, A., 2005. Immobilization of cesium in alkaline activated fly ash matrix. Journal of Nuclear Materials 346, 185–193. https://doi.org/10.1016/j.jnucmat.2005.06.006

Gasca-Tirado, J.R., Manzano-Ramírez, A., RiveraMuñoz, E.M., Velázquez-Castillo, R., Apátiga-Castro, M., Nava, R., Rodríguez-López, A., 2018. Ion exchange in geopolymers, New Trends in Ion Exchange Studies. https://doi.org/10.5772/intechopen.80970

Goni, S., Guerrero, A., Lorenzo, M.P., 2006. Efficiency of fly ash belite cement and zeolite matrices for immobilizing cesium. Journal of Hazardous Materials 137, 1608–1617. https://doi.org/10.1016/j.jhazmat.2006.04.059

Grey, I.E., Madsen, I.C., Watts, J.A., Chemistry, M., Melbourne, P., Bursill, L.A., Kwiatkowska, J., 1985. New Cesium Titanate Layer Structures. Journal of solid state chemistry 58, 350–356.

Ide, Y., Sadakane, M., Sano, T., Ogawa, M., 2014. Functionalization of layered titanates. Nanoscience and Nanotechnology 14, 2135–2147. https://doi.org/10.1166/jnn.2014.8525

International Atomic Energy Agency, 2002. Application of ion exchange processes for the treatment of radioactive waste and management of spent ion exchangers, Technical reports series No.408. Vienna.

Ito, J., 1976. Crystal synthesis of a new cesium aluminosilicate, CsAlSi5O12. American Mineralogist 61, 170–171.

Izawa, H., Kikkawa, S., Koizumi, M., 1982. Ion exchange and dehydration of layered titanates, Na2Ti3O7 and K2Ti4O9. Journal of Physical Chemistry 86, 5023–5026. https://doi.org/10.1021/j100222a036

Jang, J.G., Park, S.M., Lee, H.K., 2017. Cesium and strontium retentions governed by aluminosilicate gel in alkali-activated cements. Materials 10, 447. https://doi.org/10.3390/ma10040447

Kamalloo, A., Ganjkhanlou, Y., Aboutalebi, S.H., Nouranian, H., 2010. Modeling of compressive strength of metakaolin based geopolymers by the use of artificial neural network. International Journal of Engineering 23, 145–152.

Ke, X., Bernal, S.A., Sato, T., Provis, J.L., 2019. Alkali aluminosilicate geopolymers as binders to encapsulate strontium-selective titanate ion-exchangers. Dalton Transactions 48, 12116–12126. https://doi.org/10.1039/c9dt02108f

Khalil, M.Y., Merz, E., 1994. Immobilization of intermediate-level wastes in geopolymers. Journal of Nuclear Materials 211, 141–148.

Kirishima, A., Sasaki, T., Sato, N., 2015. Solution chemistry study of radioactive Sr on Fukushima Daiichi NPS site. Nuclear Science and Technology 52, 152–161. https://doi.org/10.1080/00223131.2014.935510

Komljenovi, M., Tanasijevi, G., D, N., Provis, J.L., 2020. Immobilization of cesium with alkali-activated blast furnace slag. Journal of Hazardous Materials 388. https://doi.org/10.1016/j.jhazmat.2019.121765

Kuenzel, C., Cisneros, J.F., Neville, T.P., Vandeperre, L.J., Yurimoto, H., Simons, S.J.R., Bensted, J., Cheeseman, C.R., 2015. Encapsulation of Cs/Sr contaminated clinoptilolite in geopolymers produced from metakaolin. Journal of Nuclear Materials 466, 94–99. https://doi.org/10.1016/j.jnucmat.2015.07.034

Lehto, J., Brodkin, L., Harjula, R., Tusa, E., 1999. Separation of radioactive strontium from alkaline nuclear waste solutions with the highly effective ion exchanger SrTreat. Nuclear Technology. https://doi.org/10.13182/NT99-A2985

Lehto, J., Clearfield, A., 1988. Preparation, structure, and ion-exchange properties of Na4Ti9O20 x H2O. Journal of solid state chemistry 73, 98–106.

Lehto, J., Clearfield, A., 1987. The ion exchange of strontium on sodium titanate Na4Ti9O20 x H2O. Journal of Radioanalytical and Nuclear Chemistry 1, 1–13.

Li, N., Zhang, L., Chen, Y., Fang, M., Zhang, J., Wang, H., 2012. Highly efficient, irreversible and selective ion exchange property of layered titanate nanostructures. Advanced Functional Materials 22, 835–841. https://doi.org/10.1002/adfm.201102272

Lizcano, M., Kim, H.S., Basu, S., Radovic, M., 2012. Mechanical properties of sodium and potassium activated metakaolin-based geopolymers. Materials Science 47, 2607–2616. https://doi.org/10.1007/s10853-011-6085-4

Mehta, P.K., Monteiro, P.J.M., 2014. Concrete: Microstructure, properties, and materials, Forth edit. ed. McGraw-Hill Education.

Nakabayashi, R., Sugiyama, D., 2017. Methodology to optimize radiation protection in radioactive waste disposal after closure of a disposal facility based on probabilistic approach. Journal of Nuclear Science and Technology 1–13. https://doi.org/10.1080/00223131.2017.1397561

Nuclear Energy Agency, 1999. Low-level radioactive waste repositories : An analysis of costs.

Nuclear Regulatory Authority of Japan, 2013. Interpretation of the NRA ordinance prescribing standards for the location, structure, and equipment of category 2 waste disposal facilities. Japan.

O'Connor, S.J., MacKenzie, K.J.D., Smith, M.E., Hanna, J. V., 2010. Ion exchange in the charge-balancing sites of aluminosilicate inorganic polymers. Materials Chemistry 20, 10234–10240. https://doi.org/10.1039/c0jm01254h

Ochs, M., Pointeau, I., Giffat, E., 2006. Caesium sorption by hydrated cement as a function of degradation state : Experiments and modelling. Waste Management 26, 725–732. https://doi.org/10.1016/j.wasman.2006.01.033

Pearson, R.G., 1988. Absolute electronegativity and hardness: application to inorganic chemistry. Inorganic Chemistry 734–740. https://doi.org/10.1021/ic00277a030

Pilarski, M., Marschall, R., Gross, S., Wark, M., 2018. Layered cesium copper titanate for photocatalytic hydrogen production. Applied Catalysis B: Environmental 227, 349–355. https://doi.org/10.1016/j.apcatb.2018.01.039

Plecas, I., Peric, A., Kostadinovic, A., Drljaca, J., Glodic, S., 1992. Leaching behavior of 60-Co and 137-Cs from spent ion exchange resins in cement matrix. Cement and Concrete Research 22, 937–940.

Provis, J.L., 2014. Geopolymers and other alkali activated materials: why, how, and what? Materials ans Structures 11–25. https://doi.org/10.1617/s11527-013-0211-5

Provis, J.L., Bernal, S.A., 2014. Geopolymers and related alkali-activated materials. Annual Review of Materials Research 44, 299–327. https://doi.org/10.1146/annurev-matsci-070813-113515

Rahman, R.O.A., Zaki, A.A., El-Kamash, A.M., 2007. Modeling the long-term leaching behavior of 137 Cs , 60 Co , and 152 , 154 Eu radionuclides from cement – clay matrices. Journal of Hazardous Materials 145, 372–380. https://doi.org/10.1016/j.jhazmat.2006.11.030

Saito, K., Fujimura, K., Sugo, T., 2018. Innovative polymeric adsorbents: Radiation-induced graft polymerization. Springer Nature Singapore Pte Ltd. https://doi.org/http://doi.org/10.1007/978-981-10-8563-5

Sakamoto, N., Itoh, S., Yurimoto, H., 2008. Discovery of 17,18 O-rich material from meteorite by direct-imaging method using stigmatic-SIMS and 2D ion detector. Applied Surface Science 255, 1458–1460. https://doi.org/10.1016/j.apsusc.2008.05.052

Sakamoto, N., Yurimoto, H., 2006. Highly sensitive ion imaging system using direct combination of a stacked-type solid-state imager and microchannel plate driven by LanVIEW softwear. Surface and Interface Analysis 38, 1760–1762. https://doi.org/10.1002/sia.2447

Shannon, R.D., 1976. Revised effective ionic radii and systematic studies of interatomie distances in halides and chaleogenides. Acta Crystallographica A32, 751–767. https://doi.org/https://doi.org/10.1107/S0567739476001551

Shi, C., Fernández-Jiménez, A., 2006. Stabilization / solidification of hazardous and radioactive wastes with alkali-activated cements. Journal of Hazardous Materials 137, 1656–1663. https://doi.org/10.1016/j.jhazmat.2006.05.008

Shi, C., Spence, R., 2004. Designing of cement-based formula for solidification/stabilization of hazardous, radioactive, and mixed wastes. Critical Reviews in Environmental Science and Technology 34, 391–417.

Shibata, T., Solo-gabriele, H., Hata, T., 2012. Disaster waste characteristics and radiation distribution as a result of the Great East Japan Earthquake. Environmetal Science and Technology 46, 3618–3624. https://doi.org/10.1021/es300055m

Skorina, T., 2014. Ion exchange in amorphous alkali-activated aluminosilicates : Potassium based geopolymers. Applied Clay Science 87, 205–211. https://doi.org/10.1016/j.clay.2013.11.003

Škvára, F., Kopecký, L., Němeček, J., Bittnar, Z., 2006. Microstructure of geopolymer materials based on fly ash. Ceramics - Silikaty 50, 208–215.

Snellings, R., Mertens, G., Elsen, J., 2012. Supplementary cementitious materials. Reviews in Mineralogy and Geochemistry 74, 211–278. https://doi.org/10.2138/rmg.2012.74.6

Takahatake, Y., Shibata, A., Nomura, K., Sato, T., 2017. Effect of flowing water on Sr sorption changes. Minerals 7, 247–260. https://doi.org/10.3390/min7120247

Tusa, E., 2014. Efficiency of Fortum's Cstreat ® and Srtreat ® in cesium and strontium removal in Fukushima Daiichi Npp, in: ENC 2014: European Nuclear Conference; Marseille (France); 11-14 May 2014. p. Paper A0020.

Tusa, E., Power, F., Oy, H., 2014. Cesium and strontium removal with highly selective ion exchange media in Fukushima and cesium removal with less selective media - 14018. WM 2014 Conference; Arizona (USA); 2-6 March 2014 1–10.

Vandevenne, N., Ion, R., Carleer, R., Samyn, P., Haen, J.D., Pontikes, Y., Schreurs, S., Schroeyers, W., 2018. Alkali-activated materials for radionuclide immobilisation and the effect of precursor composition on Cs / Sr retention. Journal of Nuclear Materials 510, 575–584. https://doi.org/10.1016/j.jnucmat.2018.08.045

Villard, A., Siboulet, B., Toquer, G., Merceille, A., Grandjean, A., Dufrêche, J.F., 2015. Strontium selectivity in sodium nonatitanate Na4Ti9O20 x H2O. Journal of Hazardous Materials 283, 432–438. https://doi.org/10.1016/j.jhazmat.2014.09.039

Walkley, B., Ke, X., Hussein, O.H., Bernal, S.A., Provis, J.L., 2020. Incorporation of strontium and calcium in geopolymer gels. Journal of Hazardous Materials 382, 121015. https://doi.org/10.1016/j.jhazmat.2019.121015

Wen, T., Zhao, Z., Shen, C., Li, J., Tan, X., Zeb, A., Wang, X., Xu, A., 2016. Multifunctional flexible free-standing titanate nanobelt membranes as efficient sorbents for the removal of radioactive 90 Sr2+ and 137 Cs+ ions and oils. https://doi.org/10.1038/srep20920

Wieland, E., Tits, J.A.N., Kunz, D., Dähn, R., 2008. Strontium Uptake by Cementitious Materials 42, 403–409. https://doi.org/10.1021/es071227y